

**ECONOMIC GEOLOGY
RESEARCH UNIT**

University of the Witwatersrand
Johannesburg

THE DISTRIBUTION OF RADIODELEMENTS IN ARCHAEOAN GRANITES
OF THE KAAPVAAL CRATON, WITH IMPLICATIONS FOR THE
SOURCE OF URANIUM IN THE
WITWATERSRAND BASIN

L.J. ROBB, M. MEYER, M.F. FERRAZ and G.R. DRENNAN

INFORMATION CIRCULAR No. 210

UNIVERSITY OF THE WITWATERSRAND
JOHANNESBURG

THE DISTRIBUTION OF RADIOELEMENTS IN ARCHAEN GRANITES
OF THE KAAPVAAL CRATON, WITH IMPLICATIONS FOR THE
SOURCE OF URANIUM IN THE
WITWATERSRAND BASIN

by

L.J. ROBB¹, M. MEYER^{1,2}, M.F. FERRAZ⁺ AND G.R. DRENNAN¹

- (1. Economic Geology Research Unit, Department of Geology, University of the Witwatersrand, Johannesburg, P.O.WITS 2050, South Africa
2. Schonland Research Centre for Nuclear Sciences, University of the Witwatersrand, Johannesburg, P.O.WITS 2050, South Africa)

present address: + Luijendaalsvlei Geological Centre, Goldfields of South Africa Limited, P.O.Box 53, Krugersdorp 1740, South Africa).

ECONOMIC GEOLOGY RESEARCH UNIT
INFORMATION CIRCULAR NO. 210

May, 1989

THE DISTRIBUTION OF RADIODELEMENTS IN ARCHAEN GRANITES
OF THE KAAPVAAL CRATON, WITH IMPLICATIONS FOR THE
SOURCE OF URANIUM IN THE
WITWATERSRAND BASIN

ABSTRACT

Approximately 500 samples from the Archaean granitic basement of the southern Kaapvaal Craton have been analysed, *inter alia*, for U and Th. When viewed in conjunction with geological relationships, the radioelement distribution patterns in the Archaean basement provide constraints regarding the origin of uranium in the Witwatersrand Basin.

Granites in the Barberton region are sub-divided into three magmatic cycles, the earliest cycle comprising tonalite-trondjemite gneisses, the intermediate cycle comprising laterally extensive K-rich batholiths and the final stage consisting of discrete intrusive granitic plutons. Uranium and thorium contents vary as a function of age and rock type, and increase progressively from the first cycle through to the third cycle. Certain of the late granite plutons may have been S-type in origin, have relatively low Th/U ratios, high U contents, and are characterized by accessory minerals dominated by monazite-like phases. The late granite plutons with the highest radioelement contents appear to have formed circa 2.8 Ga, an age which coincides with granulite facies metamorphism and uranium-thorium depletion in the lower crust, as recorded in the Vredefort crustal profile.

Granites from the hinterland of the Witwatersrand Basin are largely correlatable with the second or third magmatic cycles at Barberton. Many of these granites - protected from erosion by early Proterozoic cover sequences - preserve evidence for hydrothermal alteration. Hydrothermally altered granites are often enriched in uranium and also exhibit low Th/U ratios indicating decoupling of uranium with respect to thorium in the hydrothermal environment. In one area the Archaean basement is characterized by a zone of greisenization in which uraninite is an abundant accessory phase.

Large areas of the sub-surface Archaean granitic basement in the Witwatersrand hinterland are overlain by vestiges of apalaoregolith which may ultimately have been the source of much of the detritus in the depository itself.

Uranium has been leached from portions of the regolith profile, but also concentrated into leucoxene-rich zones derived from the breakdown of pre-existing titanium-bearing phases. The widespread development of an uraniferous leucoxene protore in weathered source rocks of the Witwatersrand Basin has relevance to the genesis of authigenic U-Ti phases (brannerite) in the reefs themselves.

In the Witwatersrand Basin the effects of the source area on reef characteristics is demonstrated by comparison between, for example, the Kimberley Reef in the East Rand and Evander Goldfields. The Kimberley Reef at Evander is not exploited for uranium and has high average Au/U ratios, reflecting a uranium-deficient source area within which numerous greenstone remnants occur. In the East Rand, the Kimberley Reef contains significantly higher uranium contents, for any value of gold, than at Evander, pointing to a more uranium-specific source. It is also evident that reefs from the upper portion of the Witwatersrand Basin are generally enriched in uraninite and brannerite, depleted in Th-bearing phases such as monazite and thorite, and, consequently, have much higher U/Th ratios than reefs lower down in the succession. This too, points either to the existence of a fertile source region that did not exist during earlier pulses of sedimentation, or to processes that were more efficient for concentrating uranium into the depository.

The study of radioelement distribution in Archaean granites adjacent to the Witwatersrand Basin provides a framework within which considerations regarding the origin of the uranium deposits in the basin can be viewed. Factors such as the secular evolution of the Archaean granitic basement, hydrothermal processes, and palaeoweathering are all considered to have played a role in the formation of the Witwatersrand deposits.

THE DISTRIBUTION OF RADIODELEMENTS IN ARCHAEOAN GRANITES
OF THE KAAPVAAL CRATON, WITH IMPLICATIONS FOR THE
SOURCE OF URANIUM IN THE
WITWATERSRAND BASIN

CONTENTS

	<u>Page</u>
1. INTRODUCTION AND OBJECTIVES	1
A. Properties and Geochemical Behaviour of Uranium and Thorium	1
B. Abundances of Uranium and Thorium in Rock-forming Minerals	1
2. URANIUM AND THORIUM CONTENT IN GRANITES OF THE BARBERTON MOUNTAIN LAND	3
A. Geological Setting	3
B. Uranium and Thorium Distribution	3
(i) Uranium and thorium abundances	3
(ii) Mineralogical controls on U and Th distribution	3
C. Radioelement Distribution in the Late Granite Plutons	11
(i) Secular distribution of uranium within the Third Magmatic Cycle	11
3. RADIODELEMENT CONTENTS OF GRANITES FROM THE HINTERLAND OF THE WITWATERSRAND BASIN	13
A. The Nature of the Archaean Granitic Basement in the Witwatersrand Basin Hinterland	13
(i) Surface outcrops	13
(ii) Sub-surface borehole intersection	13
B. Uranium and Thorium Distribution	15
C. Radioelement Decoupling in Granites from the Witwatersrand Basin Hinterland	18
(i) Greisenized granites	21
4. URANIUM IN PALAEOWEATHERING PROFILES ON THE ARCHAEOAN GRANITIC BASEMENT	21
A. Characteristics of Palaeoregolith Profiles	21
B. Uranium and Thorium Distribution	25
C. Uranium Distribution Evident from Fission Track Micro-mapping	25
5. SOME ASPECTS OF THE URANIUM DISTRIBUTION IN WITWATERSRAND REEFS	27
A. Source Area Considerations	27
B. Uranium and Thorium Distribution in Witwatersrand Reefs	27
(i) The Promise Reefs, Government Subgroup, West Rand Group	27

(ii) The Beisa Reef, Virginia Formation, Central Rand Group	30
(iii) The Kimberley Reef in the East Rand and Evander Goldfields	30
C. Comparative Mineralogy of Conglomerates on the Kaapvaal Craton	30
6. THE SOURCE OF URANIUM IN THE WITWATERSRAND BASIN	31
ACKNOWLEDGEMENTS	33
REFERENCES	33

Published by The Economic Geology Research Unit
Department of Geology
University of the Witwatersrand,
1 Jan Smuts Avenue,
Johannesburg 2001
South Africa.

ISBN 1 86814 108 X

THE DISTRIBUTION OF RADIODEMENTS IN ARCHAEOAN GRANITES
OF THE KAAPVAAL CRATON, WITH IMPLICATION FOR THE
SOURCE OF URANIUM IN THE
WITWATERSRAND BASIN

1. INTRODUCTION AND OBJECTIVES

Although a considerable amount of geochemical information has now been accumulated from Archaean granitoid terranes world-wide, a comprehensive set of data on the radioelement contents of these rocks is still lacking. By contrast, granitoids of younger age have been extensively studied for their radioelement distribution, principally for a better understanding of uranium and thorium geochemistry, but also for heat flow and isotopic studies and in the assessment of their economic potential.

Over the past four years an attempt has been made to gather data on the radioelement contents of Archaean granitoids within the Kaapvaal Craton, using the Barberton Mountain Land as a type area. The Barberton region is ideally suited for this type of study as good geological, chemical, and chronological controls exist, and an extensive sample population is available for analytical purposes. This research has been extended to include a study of radioelement contents in the granitoid basement forming the hinterland to the Witwatersrand Basin. One good reason for studying uranium distribution of the Archaean basement is the need to explain the origin of the uranium that has been so efficiently concentrated into the sediments of the Witwatersrand Basin. It is well known that uranium, as well as gold, is preferentially concentrated into the upper (Central Rand Group) portion of the Witwatersrand depository and, furthermore, that the mineralized reef horizons are characterized by very high U/Th ratios indicating that U and Th have been effectively decoupled at some stage during the processes that led to their eventual accumulation in the sediments. The object of this study is, therefore, to examine the distribution of uranium and thorium in the Archaean granitoid basement in terms of both secular and lithological variations, and to assess the extent to which these patterns may have influenced the formation of uranium deposits in the Witwatersrand Basin.

A. Properties and Geochemical Behaviour of Uranium and Thorium

Both U and Th are naturally radioactive and continually decay to form stable daughter isotopes. Naturally occurring uranium consists of three isotopes, U_{238} , U_{235} , and U_{234} , the first two of which are parent isotopes for two separate decay series which ultimately yield Pb_{206} and Pb_{207} respectively. The principal Th isotope is Th_{230} which is a product of the U_{238} decay series and is also formed by alpha decay of the insignificant U_{234} isotope.

Both U and Th are lithophile elements and are strongly concentrated into the earth's crust. In the "primary" or magmatic environment, both U and Th occur in the tetravalent form (U^{4+} , Th^{4+}) and have similar ionic radii of 0.89\AA , and 0.95\AA respectively. As such, both elements are "incompatible" in that they are not readily accepted into the lattice of major rock-forming minerals. In the "secondary" environment, however, U is very easily oxidized to the uranyl ion and accordingly, its valence state in minerals varies from U^{4+} to U^{6+} . The major uranium mineral is uraninite which, because of its ease of oxidation, has no fixed stoichiometry and varies in composition between UO_2 and U_3O_8 . Thorium is not easily oxidized and in nature occurs only in the Th^{4+} valence state; the principal thorium minerals are thorite ($ThSiO_4$) and thorianite (ThO_2), with significant amounts of Th also occurring in monazite and zircon.

As a result of these differences, the properties of U and Th in solution are markedly different. Once the tetravalent uranous ion has been oxidized to form the hexavalent uranyl ion (UO_{2+2}) it becomes highly soluble in aqueous solutions. The uranyl ion is particularly soluble in alkaline waters while the uranous ion is only soluble under very acid conditions (low pH) and is precipitated under alkaline conditions. The uranyl ion is prone to the formation of ionic complexes of which uranium phosphate (biphosphate) and uranium carbonate (bi- and tricarbonate) complexes are particularly prevalent.

In contrast, Th is not particularly soluble in aqueous solutions. These differing properties mean that in hydrothermal or surficial environments U and Th may be decoupled as U becomes extremely mobile and is redistributed in solution, while Th remains *in situ* or is transported as detrital particles.

B. Abundances of Uranium and Thorium in Rock-forming Minerals

The average abundance of U in the continental crust is approximately 3 ppm whilst that for Th is between 6-10 ppm (Wedepohl, 1969). Typical abundances of Th in granites are between 10-20 ppm, whilst 99% of felsic igneous rocks have U contents in the range 1-4 ppm. The concentration of the radioelements in mafic and ultramafic rocks is considerably lower, with typical values of Th being in the range 0.5-2 ppm and U-values being between one and two orders of magnitude lower than in acid igneous rocks.

The typical U and Th contents of both major and minor rock-forming minerals are presented in Table 1. It is apparent that neither U nor Th are able to substitute, to any significant degree, for any of the stoichiometric constituents in the major rock-forming minerals, and biotite is the mineral most capable of accommodating U into its lattice structure. In contrast some of the minor rock-forming minerals can accommodate significant quantities of both U and Th and can, furthermore, discriminate in their ability to accommodate either of the two elements into their lattice structures. The Th/U ratio, for example, has a restricted range in the major rock-forming minerals and is typically between 1-6, while the minor minerals exhibit a much broader range. Certain of these minerals are clearly U compatible (e.g. zircon and xenotime), while others accommodate considerably more Th than U (e.g. allanite and monazite). Apatite and, to a lesser extent, sphene contain approximately equal amounts of both U and Th.

TABLE 1: TYPICAL ABUNDANCES OF URANIUM AND THORIUM
IN ROCK-FORMING MINERALS

		<u>U in ppm</u>		<u>Th in ppm</u>		<u>Th/U</u>
MAJOR MINERALS	Quartz	1,7	(0,1-10)	-	(0,5-10)	(1,5)
	Feldspar	2,7	(0,1-10)	-	(0,5-10)	(1-6)
	Biotite	8,1	(1-60)	-	(0,5-50)	(0,5-3)
	Hornblende	7,9	(0,2-60)	-	(5-50)	(2-4)
MINOR MINERALS	Pyroxene	3,6	(0,1-50)	-	-	-
	Allanite	200	(30-1000)	9100	(1000-20000)	(10-20)
	Apatite	65	(10-100)	70	(15-250)	=1
	Sphene	280	(10-700)	510	(100-1000)	1,7
	Zircon	1330	(100-6000)	650	(100-10000)	0,4
	Monazite	3000	(500-3000)	125000	(2000-200000)	>25
	Xenotime	-	(300-40000)	-	-	-
Magnetite		-	(1-30)		(0,3-20)	> 1

(Notes: (1) Data from a number of sources compiled in Handbook of Geochemistry (1969), edited by K.H. Wedepohl.
(11) Ranges of concentration (in brackets) represent typical rather than extreme values).

2. URANIUM AND THORIUM CONTENTS IN GRANITES OF THE BARBERTON MOUNTAIN LAND

A. Geological Setting

Mapping of the granitic terrane both to the north and the south of the Barberton greenstone belt has delineated a diverse suite of granitic rock types (Figure 1). These granitic rocks have been broadly sub-divided into three categories termed "magmatic cycles" (Anhaeusser and Robb, 1981). The earliest cycle commenced approximately 3500 Ma ago and is characterized by leucocratic biotite trondhjemite and hornblende tonalite, as well as complex bimodal gneiss and migmatite. The tonalites and trondhjemites are pervasively foliated and their mode of emplacement is regarded as being diapiric. These rocks are commonly believed to have been derived by the partial melting of volcanic precursors similar to the metabasalts in the lowermost successions of greenstone belts.

Granites of the second magmatic cycle were emplaced approximately 3200–3000 Ma ago and comprise large, multi-component, potassium-rich batholiths that were passively emplaced into the pre-existing trondhjemite-tonalite crust. Coarse-grained, relatively homogeneous, porphyritic granites, adamellites, and granodiorites form the bulk of these complexes which are also intruded by veins, as well as small plutons, of a medium-to fine-grained granodiorite phase isotopically coeval with the main complex. In the Mpuluzi batholith (Figure 1) a prominent "Hood" phase of homogeneous, medium-grained granodiorite-adamellite forms a capapace to the main intrusion. The margins of all the batholiths are characterized by potassium-rich migmatites and gneisses which represent zones of interaction between the batholith magma and the pre-existing crust. The batholiths of the second magmatic cycle are considered to have been derived by widespread partial melting of tonalite and trondhjemite gneisses.

The third magmatic cycle is characterized by the intrusion of discrete, granitic plutons which cross-cut all other Archaean rock types in the region, and vary in age between 3200 and 2500 Ma. Most of the plutons are granitic (*sensu stricto*) in composition and typically are coarse-grained to porphyritic in texture. These plutons do, nevertheless, exhibit variations in their CaO, Fe₂O₃, rare earth and trace element contents. A few of the plutons (Dalmein, Salisbury Kop and Mliba) are granodioritic in composition, but also coarse grained to porphyritic in texture. The granodioritic group of late plutons is significantly older than the granitic suite. The two remaining bodies among the late plutons are quite distinctive, with one pluton (Cunning Moor) being tonalitic in composition and the other (Boesmanskop) comprising a well-differentiated syenite-granite complex. The late plutons cannot be characterized by a single petrogenetic model (Condie and Hunter, 1976; Robb, 1983), but are generally, regarded as having been derived by reworking of pre-existing crustal material.

B. Uranium and Thorium Distribution

Uranium and thorium contents of 253 samples from 27 individual granitoid bodies in the Barberton region have been determined by instrumental neutron activation analysis. These data are presented in Table 2, and also illustrated graphically in Figure 2.

(i) Uranium and thorium abundances

The U and Th contents of all samples analysed are displayed graphically in Figure 2 where it is apparent that U and Th abundances increase progressively from the first to the third magmatic cycles. Uranium contents range from 0,13 to 19,2 ppm and the Th values from 0,78 to 70,2 ppm.

A similar trend is observed in the plot of mean U and Th values (correction for the alpha-decay of U₂₃₈ and Th₂₃₂) for the individual granite bodies examined (Figure 3). Here it is apparent that although U and Th contents are significantly higher at the time of granite formation (i.e. between circa 3,5 and 2,5 Ga ago), the trend of increasing radioelement content with time is still evident. A number of other interesting features are also evident from the compilation of mean data in Table 3. Mean decay-corrected Th/U ratios also increase systematically from the first magmatic cycle (3,01) through to the third magmatic cycle (4,08). This trend is even more pronounced if the late granite (*sensu stricto*) plutons are considered alone (i.e. omitting the Dalmein, Salisbury Kop, Boesmanskop and Cunning Moor plutons), as they have a mean Th/U = 4,72. It is also interesting to note that a systematic increase in both Zr and Ce occurs in passing from the first through to the third magmatic cycles.

These trends are best explained by considering that the magmatic cycles defined in the region are inter-related by a process of consecutive re-working of pre-existing crustal material. This suggestion is supported by plots of radioelement abundances versus initial ⁸⁷Sr/⁸⁶Sr ratios (Meyer *et al*, 1986) which show that more primitive members of the first magmatic cycle (i.e. the Kaap Valley, Theespruit and Nelshoogte plutons) probably represent the source material from which magmas of the second cycle formed. Likewise, granites of the third cycle are likely to have originated from pre-existing crustal material derived from either of the preceding two cycles, or metasedimentary precursors (see later).

(ii) Mineralogical controls on U and Th distribution

The distribution of U and Th in each of the three magmatic cycles is shown as percentage histograms in Figure 4. For all three populations the log-transformed U and Th data exhibit a quasi-normal distribution. Skewed distribution patterns are more evident in the Th data than for U. It is also apparent that Th is bimodally distributed in the granites of the third magmatic cycle, a feature which reflects the difference between the less evolved granodioritic plutons and the highly differentiated granites (*sensu stricto*).

Considerations of U and Th distribution patterns in granites is controlled to a large extent by the radioelement-bearing phases, in particular the occurrence of accessory minerals such as zircon, sphene, apatite, allanite and monazite. The relationship between mineralogy and U and Th distribution is particularly well illustrated in ratio plots such as Zr/U versus U and Ce/Th versus Th (Figure 5a, b). In these plots a distinction exists between the tonalite-trondhjemite gneisses of the first magmatic cycle, and the various components of the second and third cycles. Rocks of the first cycle exhibit trends with variable Zr/U and Ce/Th ratios, indicating that the small variations in U and Th contents in these rocks are essentially

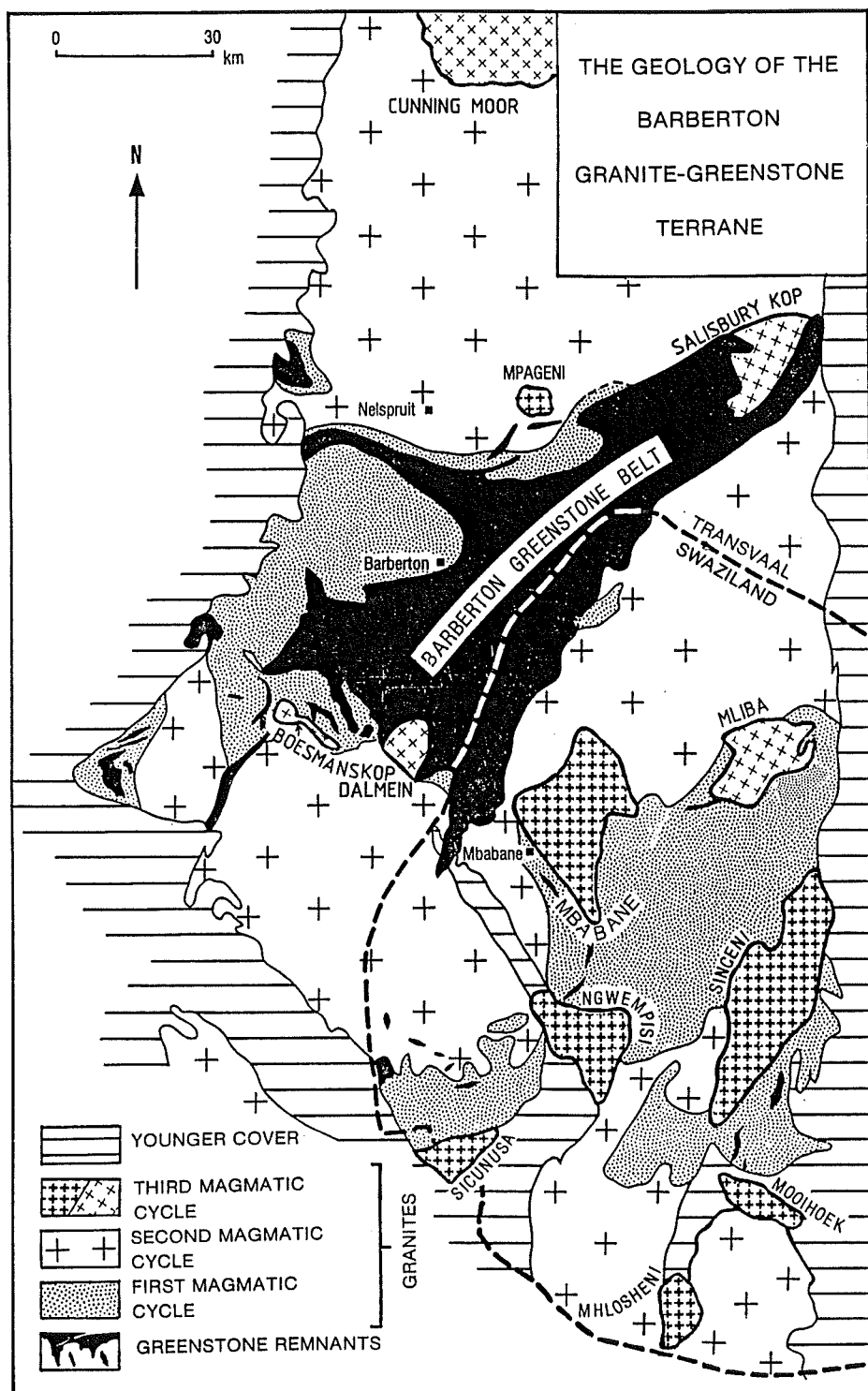


Figure 1: Simplified map showing granite types around the Barberton greenstone belt and the distribution of first, second and third magmatic cycles. Individual plutons of the Third Magmatic Cycle are named.

TABLE 2: TH AND U CONTENTS IN GRANITOIDS FROM THE BARBERTON MOUNTAIN LAND

1ST MAGMATIC CYCLE

	Th	U	Th	U	Th	U	Th	U	Th
THEESPRUIT									
TP3A	8,40	,84	ROOIHOOGLTE	1,79	,37	NELSPRUIT	14,90	,1,60	BOESMANSKOP
TP4D	3,06	,69	SY1	2,39	,74	N38	17,60	2,32	BK3
TP5	5,84	,92	SY3	1,89	,54	N11A	17,60	11,70	BK12
TP6	5,50	1,04	SM2	,78	,38	NL4	8,02	,91	BK15
TP10A	4,83	1,04	RH2	,78	N21	9,47	1,33	BK17	4,12
TP14	5,46	1,33	DOORNEHOEK		N46A	16,10	1,02	BK24	2,50
TP15	3,27	,95			K43	14,90	,96	L012	2,06
TP18	5,75	,98	DK7	6,84	S42	12,20	,61	LC22	6,06
TP21	3,45	,97	DK17	13,10	B7	16,20	3,48	LN1	5,10
TP22	4,14	1,18	DK22	4,56	C39	3,87	,80	MY1	2,60
TP23	5,23	,92	DK36	5,36	D28	6,10	,46	KZ1	5,10
TP25	4,49	1,09			A31B	14,10	1,08	KZ2	2,66
TP30	3,75	,71	WEERGEVONDEN		A31	7,23	,62	K24A	2,66
TP34	5,34	,83						BT112	5,32
TP36	5,62	1,16	LC2	2,39	,80	BERLIN			9,61
TP38	3,58	,81	LC21	1,69	,57			WGT1	4,20
TP39A	3,28	,89	LC27	8,66	1,51	N42	17,10	WC13	1,63
TP41	4,19	1,13	LC35	4,47	1,32	N44	20,10	10,50	10,50
TP44	5,03	1,45	LC36	8,38	,99				13,30
TP45	2,61	,90	WN5	3,90	,89	MPULIZI			
TP47	4,99	1,38	WN9	4,03	,87			SK1	4,71
TP49B	6,92	1,59	WN14A	3,76	1,05	BB5	31,70	4,90	SK2
TP50	2,77	,82				BB9A	9,47	6,35	SK3
TP52	1,25	,51	SCHAOPENBURG			BB10	17,70	9,10	SK4
TP53	3,57	1,07				BB12	13,60	2,02	SK5
TP54	4,41	,86	JV2	4,34	1,11	MF1	12,70	2,50	SK6A
TP55	4,61	,13	JV18	6,97	1,61	MF3	11,50	12,10	SK7
WN13	4,95	1,52	JV21	7,16	1,59	MF6	16,30	4,37	SK8
KAAP VALLEY									
LKV2	2,27	,67	STENTOR		OK12	7,35	,21	SK9A	1,88
LKV4	3,01	,94			OK14	7,35	,15	H71	1,39
LKV11	1,84	,51	K4	13,20	2,50	OK16	11,60	,44	H76
LKV13	1,98	,90	K7	11,10	1,04	TB3	16,40	4,12	MPG1
LKV14	1,50	,46	S43	,95	,54	TB8	8,45	,81	MPG2
LKV15A	1,22	,37	KM6	15,40	1,33	TB11	6,30	,77	MPG3
LKV23	1,32	,31	KM10	14,00	1,66	LR3	16,10	7,24	MPG4
LKV25	2,91	,50	KR2	11,20	1,09	LR4A	18,30	4,58	MPG5
LKV28	3,87	,73	KR8	9,55	,62	LR5	17,50	1,10	MPG6
LKV29	2,88	,50	BL4	1,89	,78	LR6	19,40	1,30	MPG7
SKV2	4,16	,64	HB7	8,14	,58	GM1A	15,50	7,94	MPG8
SKV5	3,59	,15				GM3	33,40	19,20	MPG9
SKV9	2,05	,61	NELSHOOGLTE			GM4	15,60	36,20	MPG10
SKV26	1,52	,41				GM6	16,60	2,08	MPG11
SKV33	2,89	,57	S60	2,06	,57	GM7	19,30	,87	MPG12
NW2	1,58	,42	TS16	1,00	,62	JG1A	22,80	,73	MPG13
						JG3	19,60	3,73	MPG14
						JG8	22,10	2,46	MBABANE
								4,67	

TABLE 2 (continued)

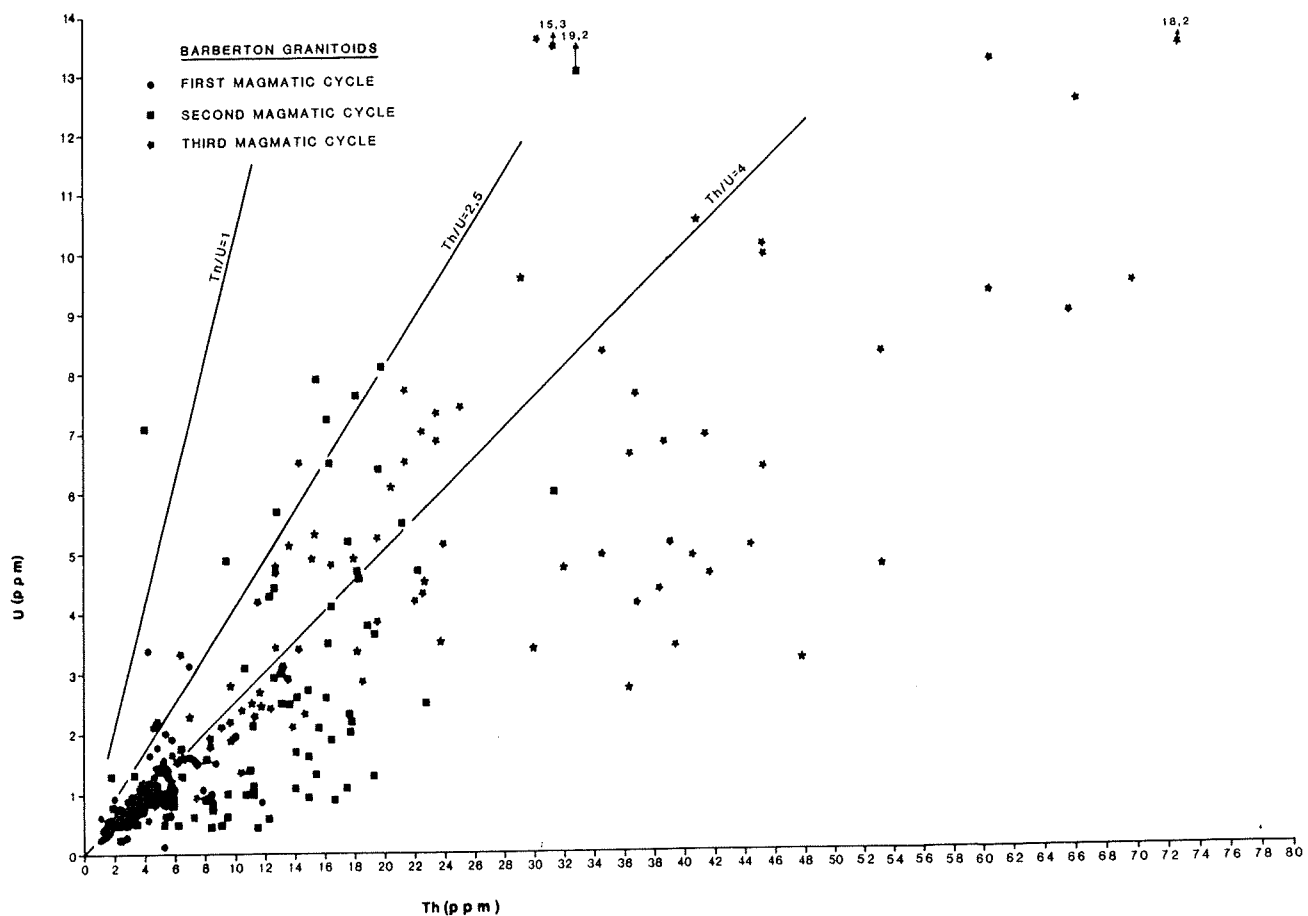


Figure 2: Plot of U versus Th for granites from the Barberton region, showing the different abundances in the first, second and third magmatic cycles.

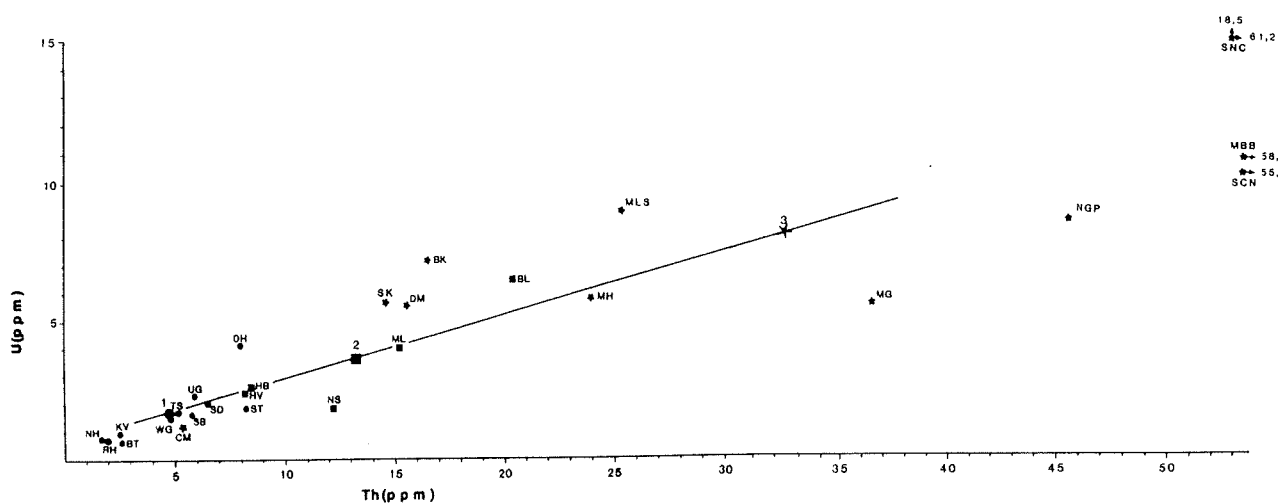


Figure 3: Plot of mean U and Th abundances for individual granite bodies sampled, corrected for the time-dependent alpha-decay of U^{238} and Th^{232} . Symbols as in Figure 2. Abbreviations provided in Table 3. Points 1, 2, and 3 are the mean decay-corrected U and Th abundances of the first, second and third magmatic cycles, respectively.

TABLE 3

Geometric Mean Th, U, Zr and Ce Contents and Geometric Mean Th and U Contents
Corrected for Alpha-decay for Individual Granite Bodies from the Barberton Mountain Land

	N	G Th(ppm)	G U(ppm)	G Th/U	G (Zr(ppm))	G Ce(ppm)	G* Th(ppm)	G* U(ppm)	G* Th/U
1st MAGMATIC CYCLE									
Theselvruit (TS)	28	4,27	0,92	4,64	126	29,7	5,08	1,56	3,46
Kaap Yallisy (KV)	16	2,24	0,57	3,93	117	34,6	2,67	0,98	2,72
Uitgevonden (UG)	6	5,74	1,47	3,90	235	67,6	6,75	2,37	2,85
Steynsdrif (SD)	6	5,41	1,22	4,43	205	52,3	6,43	2,07	3,11
Bataisia (BT)	5	2,27	0,42	5,40	132	30,4	2,61	0,64	4,08
Rooibroogte (RH)	4	1,58	0,49	3,22	152	72,9	1,86	0,79	2,35
Doorinorok (DII)	4	6,84	2,52	2,71	148	40,5	8,01	4,11	1,95
Neishoogte (NH)	2	1,44	0,59	2,44	87	26,3	1,69	0,97	1,74
Wierpoorten (WG)	8	4,03	0,96	4,16	158	61,0	4,74	1,50	3,16
Schnippeburg (SB)	5	4,83	1,01	4,73	163	53,8	5,67	1,65	3,44
Stentoor (ST)	9	7,16	1,11	6,45	216	107,0	8,23	1,82	4,52
		AVE	159	52,3	159	4,88	1,68	3,02	
2nd MAGMATIC CYCLE									
Houtenvuur (HV)	13	7,03	1,67	4,21	136	58,4	8,17	2,65	3,08
Heilvruit (HS)	13	10,30	1,15	8,36	116	94,2	12,10	1,85	6,54
Hebron (HB)	2	6,97	1,53	4,56	149	73,6	8,20	2,51	3,27
Berlin (BL)	2	18,50	3,93	4,71	277	238,0	21,80	6,44	3,39
Mauluzzi (ML)	39	13,20	2,52	4,77	208	116,0	15,30	4,00	3,82
		AVE	177	116,0	13,11	3,49	3,49	4,02	
3rd MAGMATIC CYCLE									
Dalmatin (DM)	8	13,10	3,39	3,86	198	111,0	15,40	5,54	2,78
Salisbury Kop (SK)	12	12,50	3,53	3,49	147	68,9	14,50	5,61	2,58
Boesmanskop (BK)	17	14,00	4,62	3,03	525	256,0	10,10	7,16	2,25
Jagerni (JG)	12	22,73	2,96	7,70	317	373,0	36,50	5,53	6,60
Cunning Moor (CM)	7	4,57	0,80	5,71	227	56,5	5,25	1,23	4,27
Mbabane (MBB)	5	51,20	6,99	7,32	412	392,0	58,80	10,70	5,50
Igwenipisi (NGF)	8	39,60	5,61	7,06	375	318,0	45,60	8,65	5,27
Sicunusa (SCN)	5	48,80	6,89	7,08	318	202,0	55,80	10,30	5,40
Sinceni (SNC)	7	53,20	12,10	4,40	240	185,0	61,20	18,50	3,31
Moorinok (Mi)	3	21,40	4,13	5,18	219	151,0	23,90	5,80	4,12
Mhloshezi (MLS)	6	22,40	6,29	3,56	191	150,0	25,10	8,90	2,82
	TOTAL	252	AVE	288	205,8	32,54	8,00	4,08	

G = Geometric mean

G* = Geometric mean corrected for alpha-decay

N = Number of samples

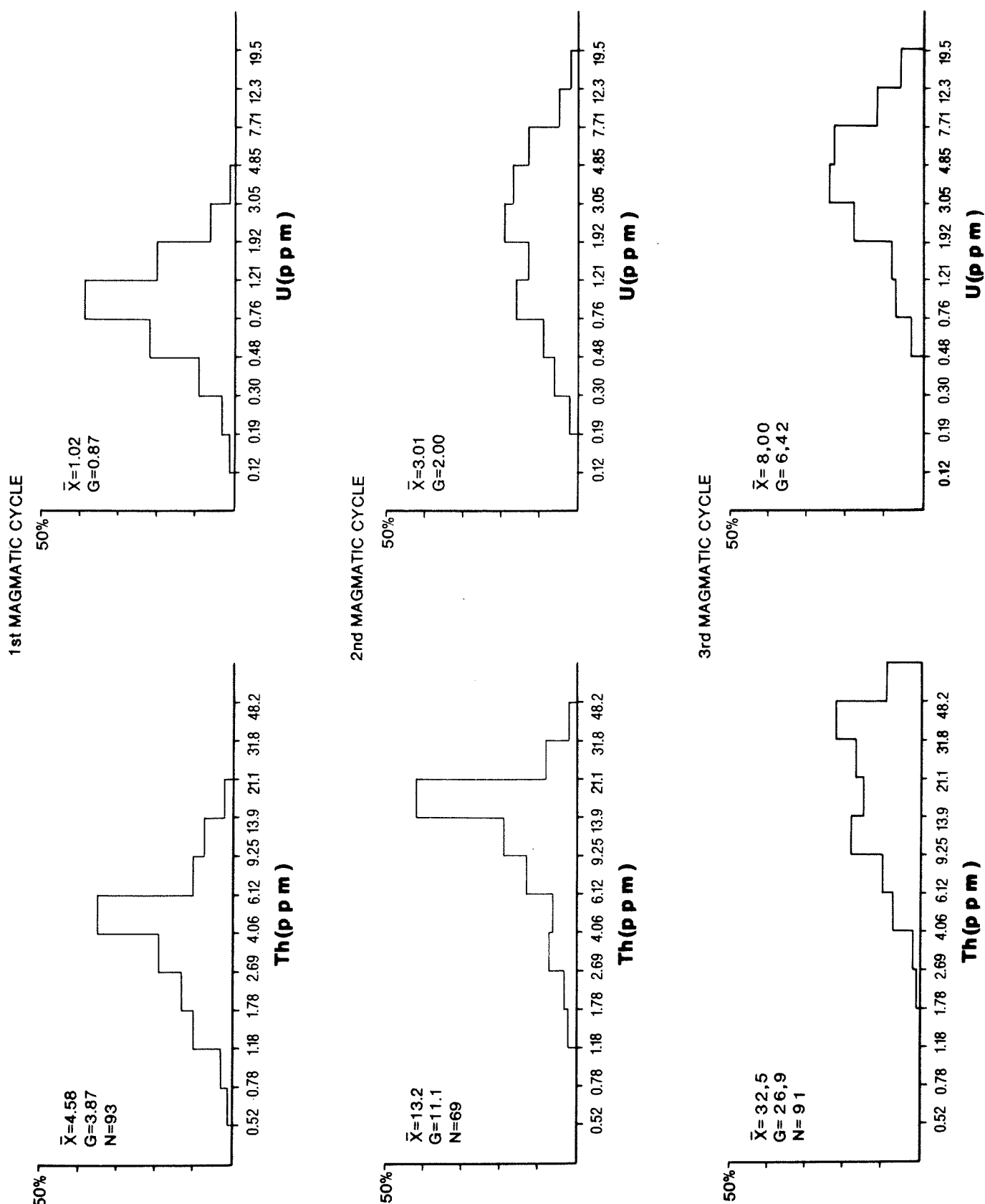


Figure 4: U and Th distribution in each of the first, second and third magmatic cycles, respectively, shown as log-transformed percentage histograms.

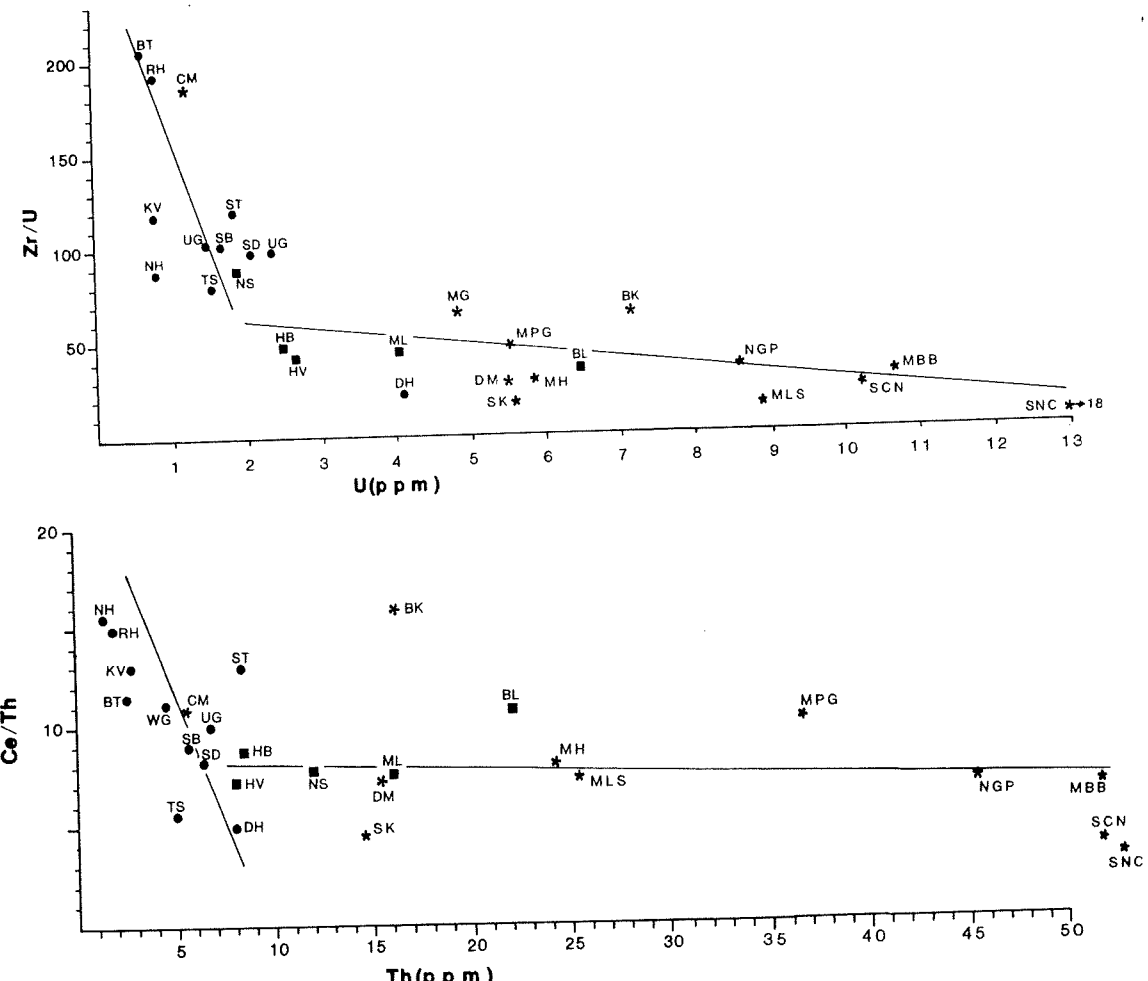


Figure 5: Plots of Zr/U versus U and Ce/Th versus Th for mean values from individual granite bodies sampled. Data and abbreviations are obtained from Table 3; U and Th mean values are decay-corrected.

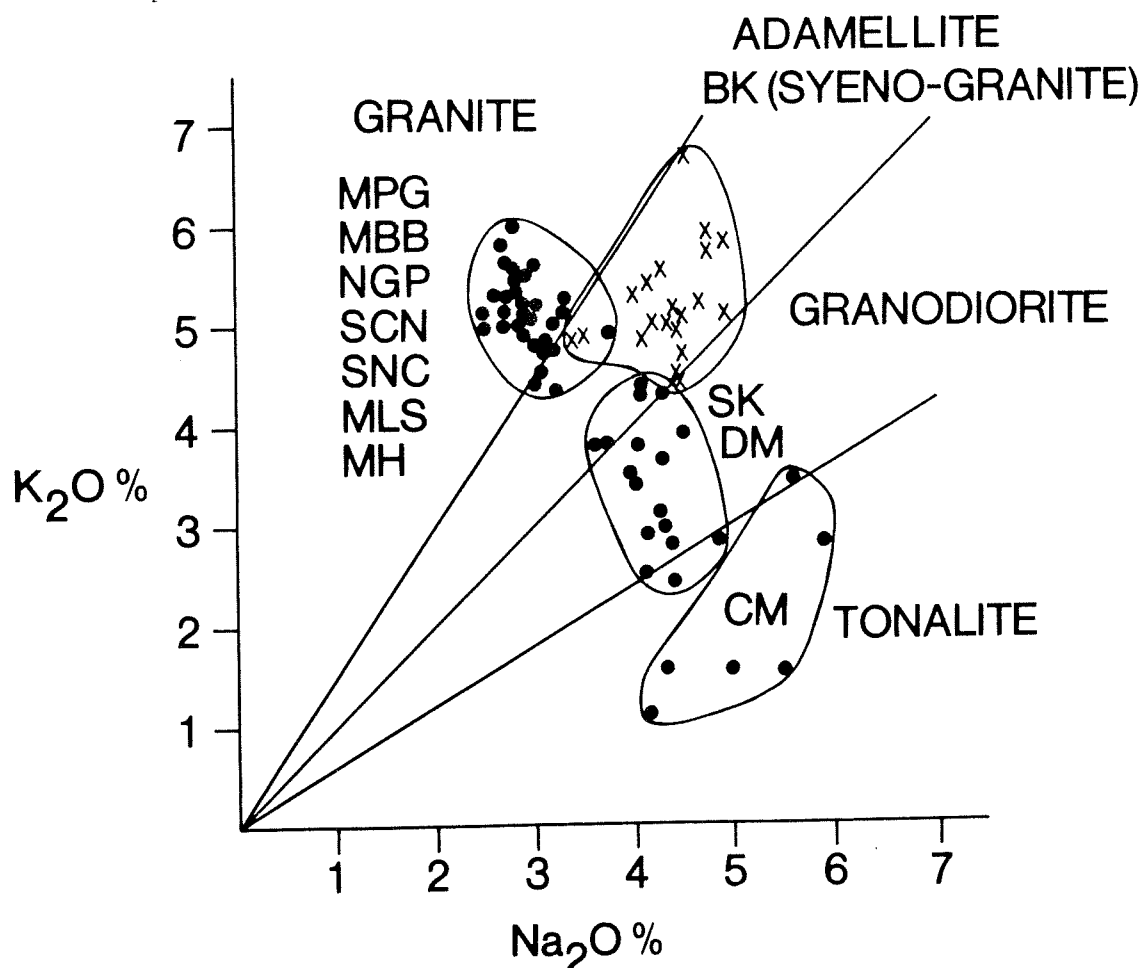


Figure 6: Plot of K_2O versus Na_2O showing the composition of individual granite plutons of the Third Magmatic Cycle. Abbreviations from Table 3.

independent of the Zr and Ce contents. Consequently, a significant proportion of U and Th in the tonalite-trondhjemite gneisses must be hosted in minerals other than the prevalent accessory phases namely biotite, hornblende, and the opaque oxides. This tendency has been confirmed by fission track techniques which indicate Th contents of up to 65 ppm in biotite and 40 ppm in hornblende from the Kaap Valley and Theespruit plutons (Vorwerk, 1984).

In contrast, the granitoids of the second and third magmatic cycles define horizontal trends along which Zr/U and Ce/Th ratios remain relatively constant. This indicates that increases in U and Th abundance are matched by concomitant increases in Zr and Ce. Hence, the distribution of radioelements in these rocks can be accounted for almost entirely by the abundances of accessory minerals such as those listed above. The lower Zr/U and Ce/Th ratios of the more evolved granite types also point to the fact that their accessory minerals contain higher U and Th contents from equivalent phases in the less-evolved granitoids.

C. Radioelement Distribution in the Late Granite Plutons

Although these granites, which comprise the Third Magmatic Cycle, are all characterized by a post-tectonic mode of emplacement, they vary significantly in age and composition. A summary of the compositional variations in the late granite plutons is presented in the K_2O versus Na_2O plot of Figure 6. Seven of the plutons, all but one of which occur in Swaziland (Figure 1), are granitic (*sensu stricto*) in composition and are highly differentiated in terms of Rb/Sr and K/Rb ratios. Three plutons are granodioritic in composition and are significantly older than the granite plutons. The two remaining plutons in the third cycle have unique characteristics, one being tonalitic in composition and the other being represented by a differentiated syenite-granite complex. In this section an emphasis will be placed on the radioelement distribution within the seven granite plutons as these have the highest U and Th contents (Figure 3).

Although the granite plutons all appear to have very similar major element compositions, detailed study indicates that they can be subdivided into two distinct subgroups. The first subgroup (Mbabane, Mpageni, Ngwempisi, Sicunusa; Figure 1) are characterized by high CaO contents (>1%), metaluminous compositions and high Th/U ratios (Table 3). Mafic minerals are dominantly biotite and hornblende. The second sub-group (Sinceni, Mooihoek, Mhlosheni; Figure 1) have lower CaO contents (<1%), lower Th/U ratios (Table 3) and compositions which transgress into the peraluminous field. Phyllosilicates consist dominantly of biotite with minor muscovite.

In addition to the above differences, the two granite subgroups are very clearly distinguished in terms of their accessory mineral assemblages. The high-CaO group is characterized by a very distinct and abundant suite of accessory minerals consisting predominantly of sphene and allanite (Figures 7b, c), together with lesser zircon, apatite (Figure 7a) and magnetite. This assemblage is entirely different to that observed in the low-CaO group where the accessory mineral assemblage is dominated by a hydrated Ca-LREE-silicophosphate phases which are isostructural with monazite (Figure 7d) as well as lesser zircon, apatite, and Fe-Ti oxides. The differences in the two groups strongly suggest that the low-CaO granites have an S-type origin, whereas the high CaO granites have I-types characteristics.

The above observations have interesting implications for the suitability of the various late plutons, either as hosts for endogenous hydrothermally derived uranium deposits, or as source rocks for exogenous uranium accumulations in sedimentary environments. Detailed work in uraniferous granitoids of the Hercynian orogeny indicates that most fertile granitoids, and those within which U mineralization is most often associated, are represented by the low-Ca, peraluminous suite (Cuney and Friedrich, 1987). Within this suite the monazite group accessory minerals predominate, and also act as an important host for uranium. If the magma is characterized by low Th/U ratios, however, low-Ca, peraluminous granites will crystallize abundant uraninite, a feature which characterizes this category of granite more than any other. Low-Ca, peraluminous granites represent important hosts for endogenous hydrothermally derived uranium deposits, although similar deposits may also form in highly differentiated, particularly peralkaline, granite types. However, the peraluminous suite undoubtedly represent the most important granite type as far as a source for uranium hosted in sedimentary deposits is concerned. This is because peraluminous granites are either capable of providing detrital uraninite in the case of anoxic environments where quartz-pebble conglomerate placers are forming, or labile uranium in the case of oxygenic environments, where uraninite is the most easily leachable source of uranium by oxidizing solutions (Cuney and Friedrich, 1987).

Among the Swaziland granite plutons, the Sinceni body (and to a lesser extent the Mhlosheni pluton) stand out as having low-Ca, low Th/U and relatively high U contents (Table 3). The Sinceni pluton is also characterized by a zone in which prominent quartz-albite tourmaline-cassiterite hydrothermal veins are developed. The pluton probably, therefore, also has a potential for vein-related uranium mineralization. Furthermore, the low-Ca suite as a whole could represent a viable source rock for early-Proterozoic quartz-pebble conglomerate placer accumulations, as well as for Phanerozoic, tabular sandstone-related deposits possibly hosted in adjacent Karoo sediments.

(i) Secular distribution of uranium within the Third Magmatic Cycle

The individual granite bodies which make up the Third Magmatic Cycle exhibit a considerable range in ages, (i.e. 3,2-2,2 Ga) although many of the age estimates in this range are relatively imprecise (Barton et al., 1983a, b). A plot of the decay-corrected U and Th contents of each of the granite bodies of the third cycle versus apparent age (Figure 8), reveals an interesting dependence of radioelement distribution on time. It would appear that granites forming in the relatively restricted interval between ca. 2,9 and 2,7 Ga were enriched in both uranium and thorium with respect to granites forming either before, or after this interval. This trend is also apparently independent of the origin of the granites in question as the bodies which define the radioelement peak have both S- and I-type characteristics (i.e. the peak being defined by the Ngwempisi, Mbabane and Sinceni granite plutons). This observation is considered potentially important in the light of data from the Vredefort structure (Figure 9), where a vertical crustal profile through approximately 15 km of the Archaean granite basement is revealed on edge. Detailed isotopic studies at Vredefort indicate that the lower crust (ca. 3,5 Ga old) was affected by an isotopic resetting event at circa 2,8 Ga, during which time strong uranium depletion associated with prograde granulite facies metamorphism is thought to have occurred (Welke and Nicolaysen, 1981). The granulite facies metamorphism and dehydration of the lower crust is considered to have been facilitated by the upward migration of volatile and U-bearing fluids which "... provided the source

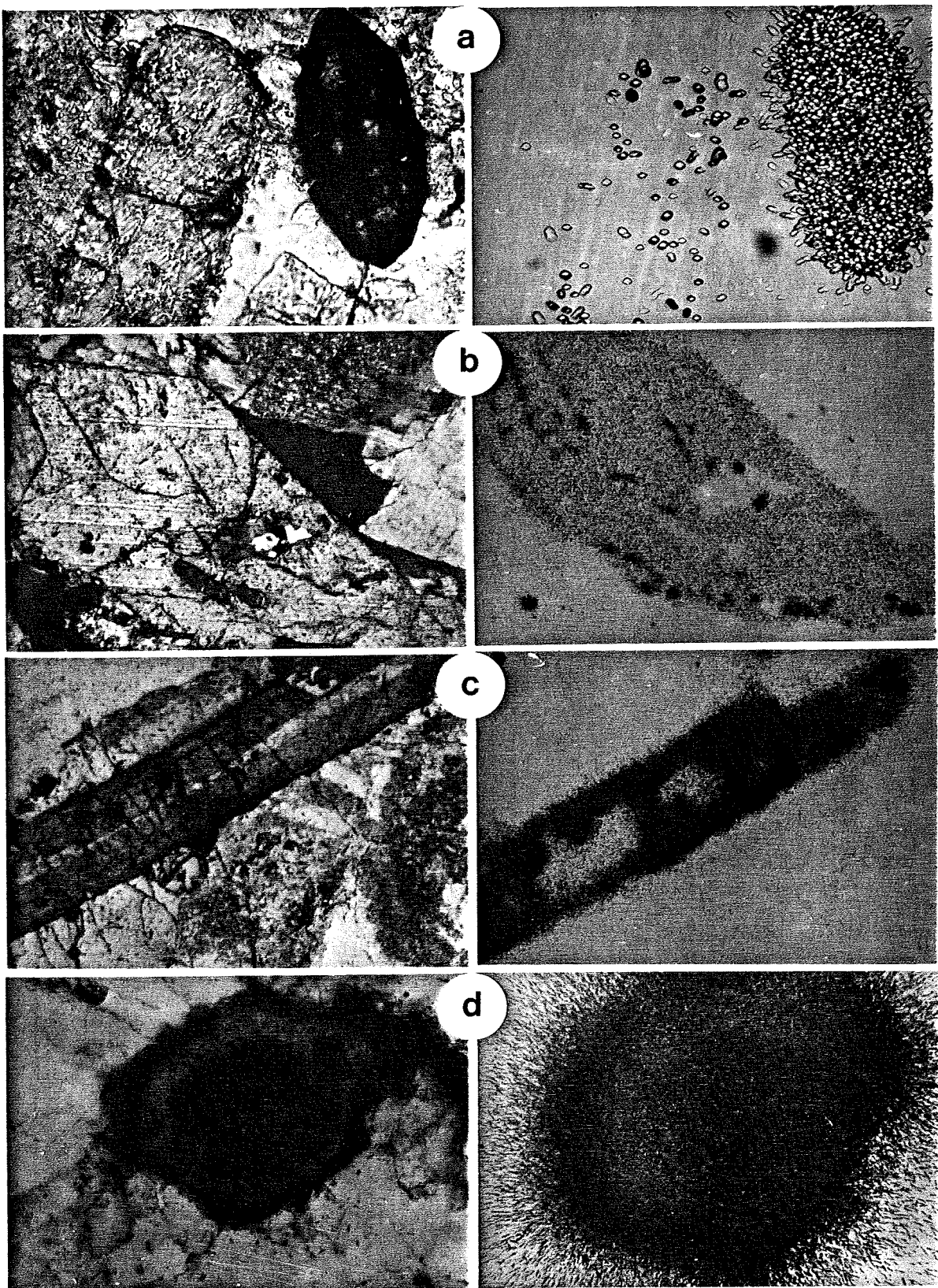


Figure 7: URANIUM DISTRIBUTION IN GRANITES FROM THE BARBERTON REGION

- a. Zircon and apatite - the two most common accessory minerals in most of the Archaean granites studied - and the accompanying fission track print showing the relative distribution of uranium in the two phases. Field of view = 0,4 mm.
- b. Sphene from the high-Ca variety of the late granite plutons, exhibiting a uniform distribution of uranium throughout the grain. Width of field of view in this and all other microphotographs is 1mm unless otherwise stated.
- c. Zoned allanite from the high-Ca variety of the late granite plutons, showing a strong concentration of uranium towards the outer portions of the grain.
- d. Metamic monazite-like phase (Ca - LREE - silicophosphate) from the low - Ca variety of the late granite plutons. This phase represents the dominant accessory mineral in the low - Ca granites. Field of view = 0,4mm.

of uranium in cross-cutting granite plutons of 2700 My age in other parts of the Kaapvaal Craton" (Hart, *et al.*, 1981). The suggestions emanating from the Vredefort study would appear, therefore, to receive strong support from the secular dependence of uranium distribution in the granitoid plutons of the Third Magmatic Cycle. In the Barberton region, the U and Th peaks between 2,9 and 2,7 Ga are possibly also related to devolatilization of the lower crust, which affected the U and Th tenor of the magmas forming at this time. Furthermore, these anomalous radioelement concentrations appear to be largely independent of the source material from which the magmas were derived, but may be related instead to the particular processes affecting large parts of the craton at that time. This concept is considered in more detail later.

3. RADIOELEMENT CONTENTS OF GRANITES FROM THE HINTERLAND OF THE WITWATERSRAND BASIN

In the Witwatersrand hinterland region, a number of domal exposures of the Archaean granitoid basement occur (Figure 9) and, although generally very poorly outcropping, these have been examined and sampled where possible. In addition, approximately 200 boreholes, that have intersected the Archaean basement beneath overlying sedimentary and volcanic sequences, have also been sampled from 10 discrete areas in the Witwatersrand Basin hinterland (Figure 9). A total of 187 samples from this region have been analysed for their U and Th abundances (Table 4), and these provide an additional dataset which supplements that from the Barberton Mountain Land and facilitates a comparison between the two regions.

A. The Nature of the Archaean Granite Basement in the Witwatersrand Basin Hinterland

(i) Surface outcrops

The distribution of exposed "windows" of the Archaean granite-greenstone basement is shown in Figure 9. Of these, the Johannesburg dome is the best exposed and has received much attention in the past (Anhaeusser, 1973, 1977, 1978). Greenstone remnants are preserved in the southern portion of the dome and consist of mafic-ultramafic volcanic and intrusive rocks very similar to the lower portions of the circa 3,5 Ga old Onverwacht Group in the Barberton greenstone belt. Granitic rocks include mesocratic hornblende-biotite tonalite gneisses and leucocratic trondhjemite gneisses and migmatites, as well as a centrally disposed zone comprising massive, homogeneous adamellites and porphyritic granites. Tonalitic gneisses have yielded a U-Pb zircon age of 3170 +/- 34 Ma (Anhaeusser and Burger, 1982) while the more potassic rock types from the centre of the dome provided a Pb-Pb whole rock age of 3060 +/- 30 Ma (Barton *et al.*, 1986).

The remaining Archaean basement domes have not been studied in as much detail, although it is clear that a wide range of granite types and textures exist. The Devon dome, which crops out between the East Rand and Evander Goldfields (Figure 9) comprises mainly granodiorites as well as strongly foliated migmatitic gneisses. West of the Johannesburg dome, the Doornfontein dome is underlain by coarse-grained, porphyritic granite while the small De Pan outlier consists mainly of a complex suite of foliated, often migmatitic tonalite gneisses. These rocks have yielded a whole rock Pb-Pb age of 3015 +/- 40 Ma (Barton *et al.*, 1986).

The Westerdam dome comprises homogeneous, medium- to coarse-grained granodiorite which has been dated at 2810 +/- 200 Ma (Barton *et al.*, 1986). The Hartbeesfontein dome consists of medium- to coarse-grained adamellite which, in places, is moderately foliated. The Ottosdal-Coligny dome consists of an unusual, reddish, leucocratic adamellite in its northern portions and a medium-grained, grey adamellite in the south. The Schweizer-Reneke dome in the far western Transvaal is fairly well exposed and reveals a suite of granites (*sensu stricto*) of varying textural character. These granites are pervasively altered in the northern portion of the dome, and also strongly foliated adjacent to a major shear zone which bisects the dome from NNW to SSE. The Schweizer-Reneke granite has yielded a Pb-Pb whole rock age of 2870 +/- 70 Ma (Barton *et al.*, 1986).

The diverse nature of the granite exposed in the domal outcrops of Archaean basement in the hinterland region are emphasized in the plot of Rb versus Sr, in Figure 10. It is clear that most of the individual domal outcrop areas are characterized by a distinctive trace element fingerprint, although certain of the domes (e.g. Johannesburg, Ottosdal-Coligny) consist of more than one phase and/or textural variant. Although the exposed granites in the Witwatersrand hinterland are compositionally diverse, it appears that they exhibit a relatively simple bimodal age distribution pattern (Barton *et al.*, 1986). These ages are circa 3,1-3,0 Ga for the sodic varieties and approximately 2,8 Ga for the more differentiated, potassic granites. Single detrital zircon dates from several Dominion and Witwatersrand conglomerate horizons indicate a wide variety of source material ranging in age from 3,2-2,9 Ga (Robb *et al.*, 1989).

(ii) Sub-surface Borehole Intersections

Borehole core has been sampled from 10 discrete areas that extend over much of the region immediately adjacent to the Witwatersrand Basin (Figure 9). This core has sampled portions of the granite basement that in many cases have remained blanketed by sedimentary or volcanic cover sequences since at least Transvaal times, and have not, therefore, been eroded to the same extent that surface basement exposures may have been. Like the surface granites, the material intersected in borehole core is compositionally diverse, and, in addition, is often characterized by an overprint of hydrothermal alteration that is not evident to the same extent in the more deeply eroded surface samples (Robb and Meyer, 1985). This suggests that in certain areas borehole core may have sampled the upper portions of roof-zones of granite bodies which, in exposed segments of the Archaean crust (e.g. Barberton), may have been largely eroded away. Three types of hydrothermal alterations are recognized in the subsurface hinterland granites. Firstly, many of the samples examined are characterized by pervasive alteration of mild intensity which involves the breakdown of pre-existing mafic minerals (principally biotite and to a lesser extent hornblende) to propylitic assemblages comprising chlorite +/- epidote +/- leucoxene. In addition, primary magmatic feldspars, in particular plagioclase, show varying degrees of alteration involving sericite, pyrophyllite, saussuritic assemblages, and in some instances, carbonate and argillitic minerals. The pervasive alteration seen in many of the samples is probably of deuterian derivation and related to near-magmatic sub-solidus processes, although in certain cases it may also be related to a lower-temperature overprint associated with the influx of meteoric fluids derived from the diagenesis of overlying sediments (Klemd *et al.*, 1986).

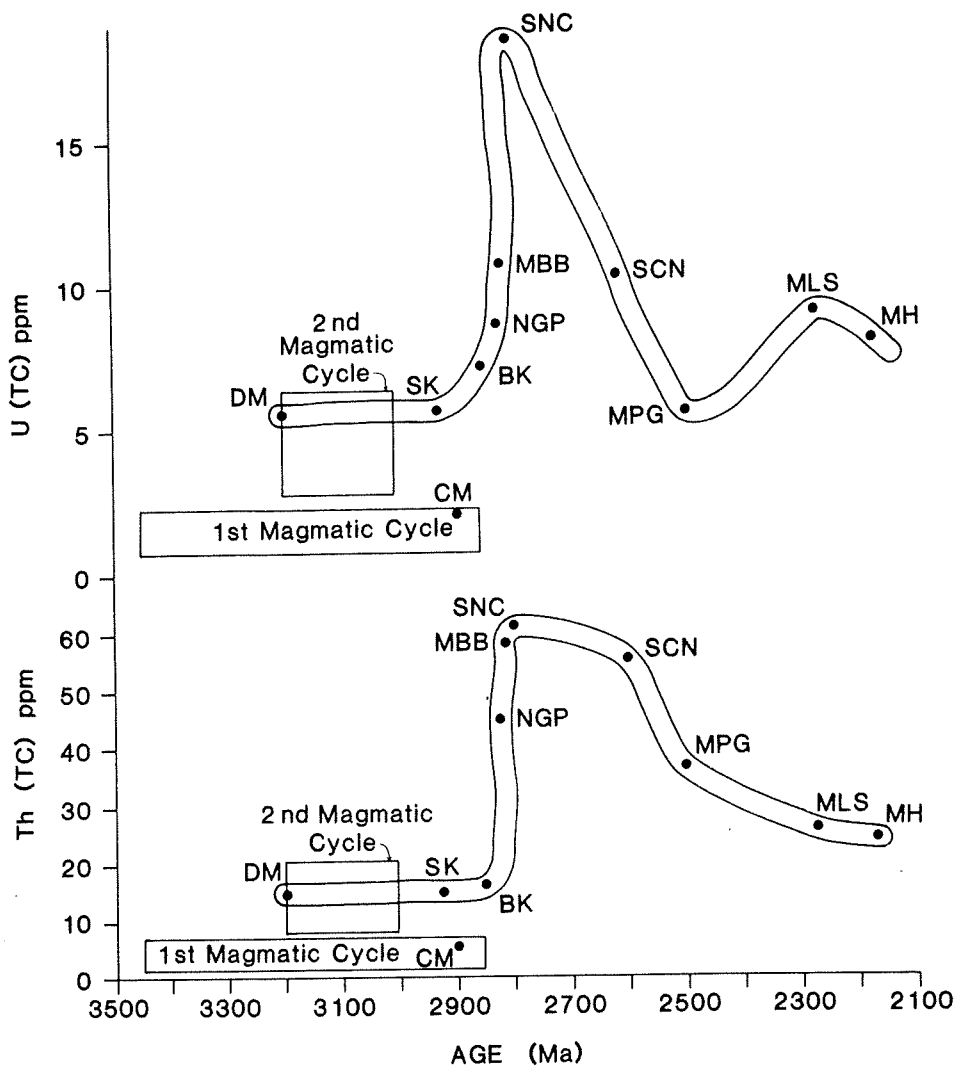


Figure 8: Plot of mean, decay-corrected U and Th contents of individual granite plutons of the Third Magmatic Cycle versus age of the pluton. Data and abbreviations from Table 3. Age data obtained from Barton (1982) and Barton et al. (1983).

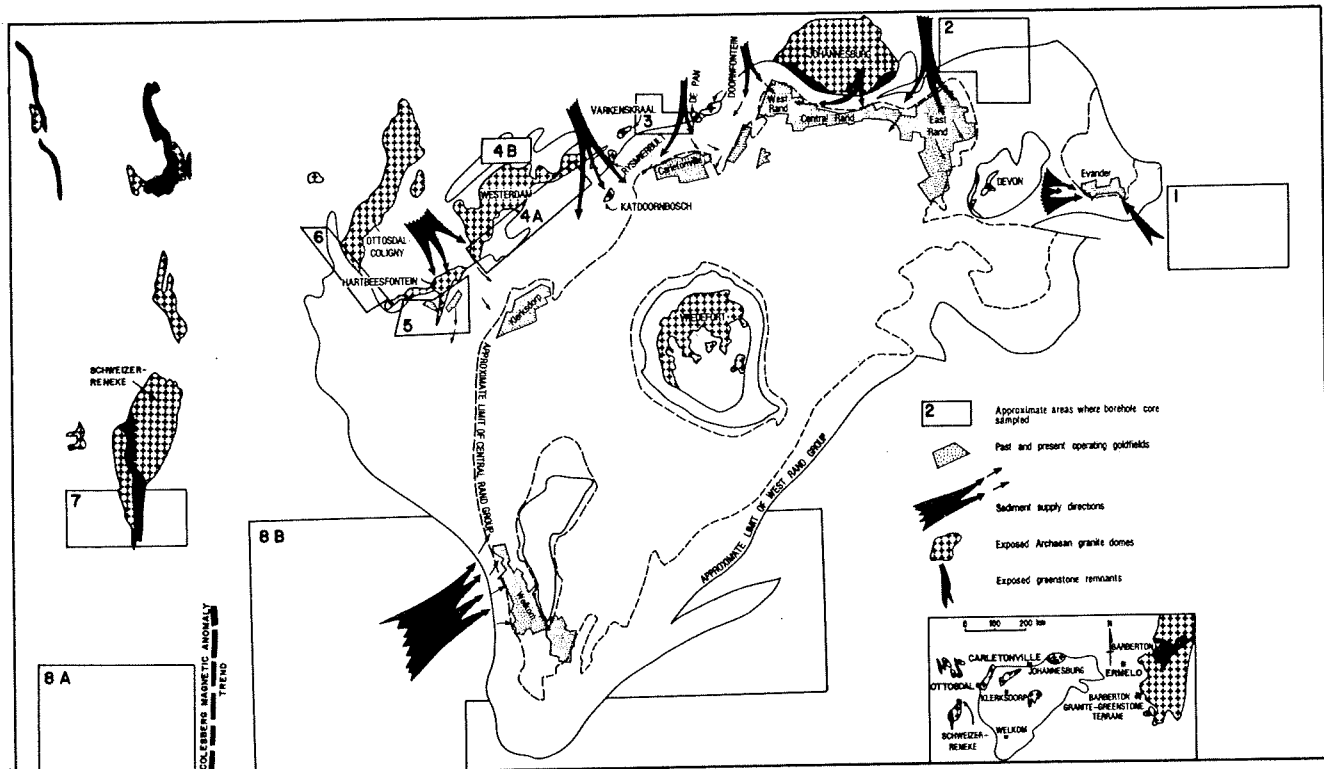


Figure 9: Schematic map showing the outline of the Witwatersrand Basin in relation to exposures of adjacent granite domes and to areas where borehole cores intersecting the Archaean basement have been sampled. The location of operating goldfields and approximate sediment supply directions are also shown.

Secondly, and of far greater significance to the question of the nature of the basement granites in the hinterland area, is the presence of vein type alteration systems in many of the borehole cores examined. The existence of veins possibly implies processes such as retrograde boiling, hydraulic fracturing and the precipitation of incompatible elements from an evolved aqueous fluid. In the study area as a whole the nature of the vein-fill and the mineral parageneses are variable and diverse. Many veins comprise quartz-sulphide or quartz-carbonate-sulphide mineralization. The carbonate phase is usually calcite although siderite has been observed, and in addition to pyrite as the dominant sulphide species, chalcopyrite, pyrrhotite, sphalerite, and molybdenite have been noted. Other vein-fill includes pneumatolytic assemblages such as fluorite-quartz-pyrite and quartz-carbonate-fluorite-sulphide. Amongst the more unusual veins are included quartz-hematite-chalcopyrite and quartz-carbonate-pyrrhotite-chalcopyrite assemblages.

A third type of alteration noted is the pervasive greisenization of a dominantly peraluminous suite of granites that occur mainly in a region to the northwest of the Klerksdorp Goldfield (Figure 9). The main feature of this style of alteration is the extensive replacement of pre-existing quartz and feldspar by an intimately intergrown, coarse-grained, quartz-muscovite assemblage. The partial albitionization of microcline to weakly-sericitized plagioclase feldspar often accompanies the greisenization. Greisens are also characterized by discrete veins of quartz-fluorite-pyrite-carbonate and quartz-chlorite-molybdenite. Also observed, commonly in juxtaposition with sulphides, are rounded to elongate carbon nodules within which uraninite is occasionally associated. Many of the peraluminous granites in this area contain primary garnet which becomes progressively altered to nodules of chlorite-carbonate-sericite towards the greisenized zones. The greisenizing process itself is related to the evolution of fairly high temperature ($>400^{\circ}\text{C}$) brines from a crystallizing granitic magma (Robb, 1987).

Although it is apparent from the nature of both the surface and subsurface basement samples that the hinterland area is composed almost entirely (i.e. $>90\%$) of granitoid rocks with very few greenstone remnants preserved, one area is notably different. The hinterland region to the Evander Goldfield (i.e. Area 1, Figure 9) is underlain by a significant component of mafic rocks which have been correlated, either with the greenstones of the Swaziland Sequence, or the mafic volcanics of the Pongola Group (Ferraz *et al.*, 1986). The unusually high preponderance of greenstone and other mafic remnants in this region has been offered as a possible explanation for the fact that the Kimberley Reef in the Evander region is generally very poor in uranium, has high chromite:zircon ratios, and is also characterized by unusually high platinum group element concentrations. Many of the granitoids in the Evander hinterland are tonalitic in composition and also, therefore, contain low radioelement contents (Ferraz, 1989; Table 4).

The suggestion that many of the subsurface granites sampled in this study are high-level intrusions with associated hydrothermal alteration, is also not applicable to the entire hinterland region. The Evander hinterland region is, again, characterized by granites lacking evidence for hydrothermal alteration. It is also now apparent that a significant proportion of the granitoid basement to the west of the Welkom Goldfield is characterized by a high-grade gneissic suite which is lower crustal in origin (Drennan *et al.*, 1988). These characteristics are evident in the area to the west of the Colesberg Magnetic Anomaly Trend (Corner *et al.*, 1986; Figure 9), where borehole core and extensive underground exposures of the Archaean basement in the Kimberley and Koffiefontein diamond mines, reveal the presence of a regionally developed suite of tonalitic-to-dioritic gneisses and migmatites. This suite of rocks is ~ 3.25 Ga old (Drennan *et al.*, 1988) and has been exposed in suboutcrop beneath the Dwyka Group by shallow eastward tilting of the crust in this region. This tilting is evident from the geophysical modelling of the Colesberg Magmatic Anomaly Trend, which also reveals that it is very similar in character to the mid-crustal magnetic anomaly that is exposed in the Vredefort dome (Corner *et al.*, 1986). It is evident from exposures at the Koffiefontein diamond mine, that this gneissic-to migmatitic basement has been also intruded by a highly differentiated granite pluton, the age of which is, at present, unknown.

B. URANIUM AND THORIUM DISTRIBUTION

The results of Th and U analysis for 187 samples of the Archaean granitoid basement in the Witwatersrand Basin hinterland are presented in Table 4 and also plotted in a U versus Th scattergram in Figure 11. A number of interesting characteristics of the Witwatersrand hinterland granitoids are evident in the U versus Th plot. The samples from areas 7 and 8A (Figure 9), which are derived from the area west of the Colesberg Magnetic Anomaly Trend, are markedly depleted in radioelements by comparison with other granites from the region. Most uranium contents in this suite are <1 ppm, and the rocks generally have high Th/U ratios (>5). Such characteristics accord with the suggestion that this segment of the basement may be lower crustal in character (Drennan *et al.*, 1988). These characteristics are also analogous to, but not as severe as, the U and Th depletion evident in the lower crustal portion of the Vredefort profile (Hart *et al.*, 1981). It is evident that most of the granite samples from the Schweizer-Reneke granite, in particular those from the northern segment of the dome (Figure 9) also have very low U contents, but high Th abundances (Table 4) and U/Th ratios. The Schweizer-Reneke granite is an evolved granite body that is characterized by moderately high Rb/Sr ratios (Figure 10) and should be expected to contain higher than normal abundances of both uranium and thorium. As this is not the case it is possible that labile uranium may have been selectively removed during the hydrothermal alteration that is evident, particularly in the northern portion of the Schweizer-Reneke dome (Robb and Meyer, 1985).

In contrast to the above characteristics, many of the samples from the hinterland granites have low Th/U ratios and may, therefore, be enriched in U relative to Th. Figure 11 shows that at least one third of the sample population from the hinterland region lies above the $\text{Th}/\text{U} = 2.5$ line, and have Th/U ratios that are less than 2.5. This is markedly different to the Barberton data where the great majority ($>90\%$) of samples have $\text{Th}/\text{U} > 2.5$. It is apparent, therefore, that many granites in the Witwatersrand Basin hinterland were either formed from magmas that initially had low Th/U ratios, or have been affected by processes, such as hydrothermal alteration, which have decoupled the radioelements and resulted in an enrichment of U relative to Th. Amongst samples from surface exposures of the granite basement it is clear that most have fairly typical radioelement contents with only a few samples from the 3060 Ma old porphyritic granites in the central portion of the Johannesburg dome showing high radioelement contents and low Th/U ratios. Particularly striking insofar as the enrichment of U with respect to Th is concerned, is the suite of greisenized, peraluminous granites from the area northwest of the Klerksdorp Goldfield (Area 5; Figure 9). Most of these granites have Th/U ratios > 2.5 and many of the severely greisenized samples generally have U in excess of Th (Figure 11). Several

— THE WILMINGTON —

Sulfur in 39m

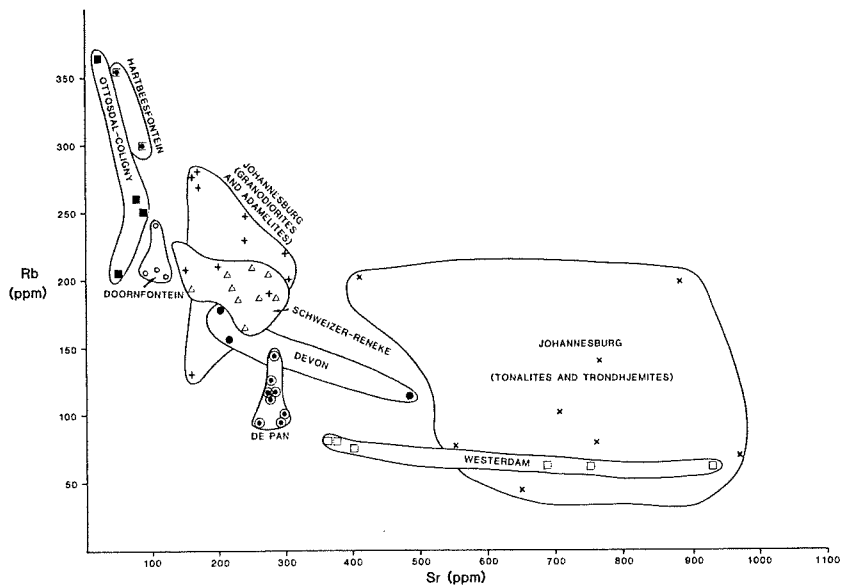


Figure 10: Plot of Rb versus Sr for individual granite domes exposed along the margins of the Witwatersrand Basin.

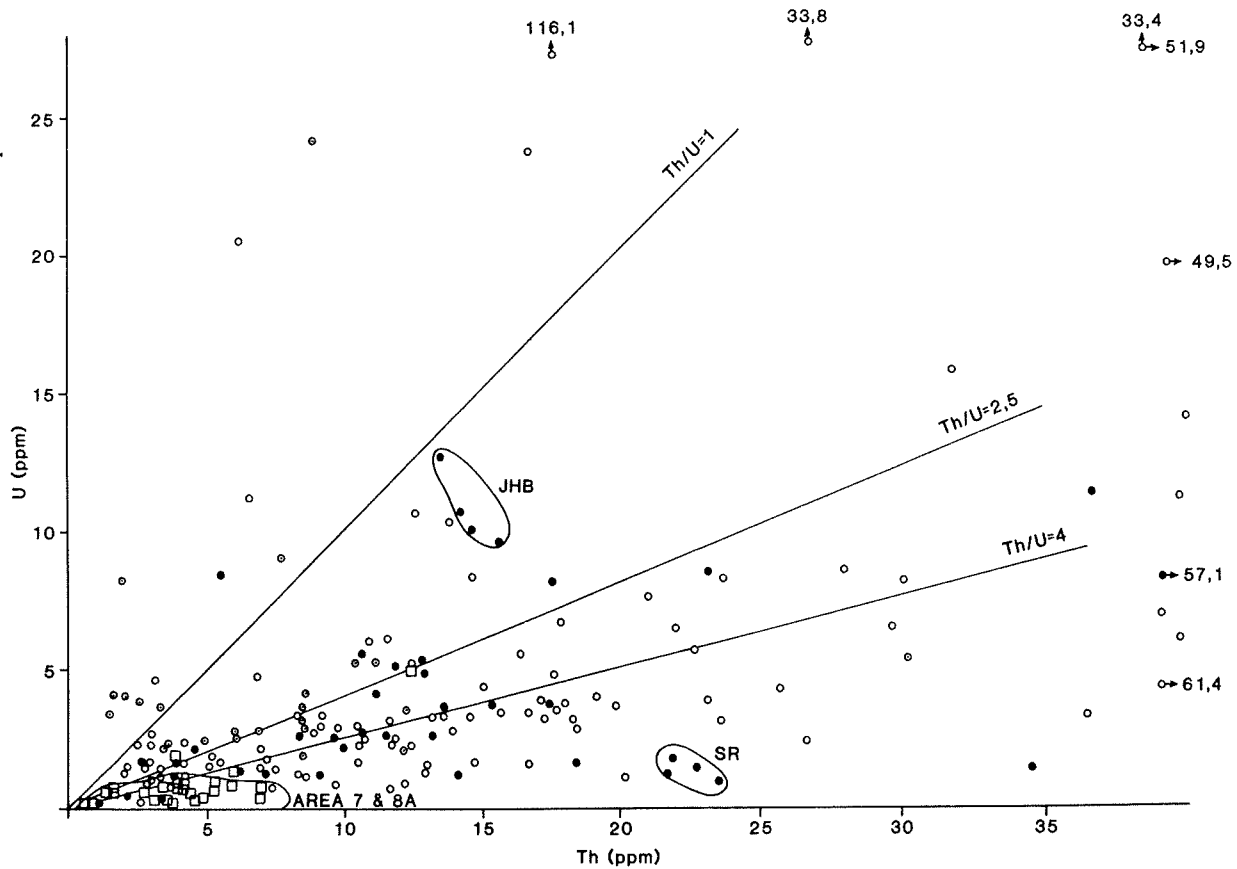


Figure 11: Plot of U versus Th for granites adjacent to the Witwatersrand Basin. Dots - surface exposures; open circles - borehole core; open squares - borehole core from areas 7 and 8a, west of the Colesberg Magnetic Anomaly Trend (Figure 9); open circles with dots - borehole samples, often greisenized, from area 5 (Figure 9). Fields JHB and SR, refer to anomalous samples from the Johannesburg and Schweizer-Reneke domes, respectively.

of the greisenized samples are so depleted in Th that they do not contain any of the typical thorium-bearing accessory minerals (such as allanite, sphene and monazite) that normally characterize granites, and uranium tends to reside almost entirely in uraninite (see later).

Certain of the granites from the Witwatersrand Basin hinterland differ markedly from those occurring in the Barberton region. These differences are discussed in more detail in the following section where emphasis is placed on the mineralogical siting of uranium, as evident from detailed fission track micro-mapping.

C. Radioelement Decoupling in Granites from the Witwatersrand Basin Hinterland

Most granites contain a typical suite of accessory minerals (which includes zircon + apatite +/- sphene +/- allanite +/- monazite-like phases) within which most (usually >80%) of the U and Th is hosted (Figure 8). As mentioned earlier, the chemical characteristics of the granitic magma (i.e. Ca activity, Si saturation, peralkalinity index, etc.) determine the specific nature of the accessory mineral suite occurring in a particular granite (Cuney and Friedrich, 1987; Sawka and Chappell, 1986). In general the solubilities of the common accessory mineral phases in a granitic melt are low, so that these phases will crystallize early and thereby control the partitioning of U and Th during crystallization of the magma. By contrast, during subsequent hydrothermal processes the solubility of many of the common accessory minerals with respect to the fluid phase, is high (in particular monazite, sphene, allanite, and apatite), and these phases will dissolve and liberate U and Th (Cathelineau, 1987). Uranium in particular, becomes prone to oxidation and to complexing by ligands such as CO_3^{2-} , PO_4^{3-} , and the halogenides, and is, therefore, easily transported by hydrothermal solutions. In many of the hinterland granites detailed fission track micro-mapping provides convincing evidence for the mobilization of uranium during hydrothermal alteration of these rocks, and its subsequent precipitation in, or around, suitable subsolidus mineral assemblages.

Even in rocks that are only mildly altered, there is an indication that uranium has been mobilized and reconcentrated into certain of the subsolidus mineral phases. Most of the hydrothermally altered granites in the hinterland region undergo pervasive propylitization, which results in the breakdown of biotite and/or hornblende to an assemblage comprising chlorite + leucoxene +/- magnetite/ilmenite +/- epidote +/- a carbonate mineral. Low levels of uranium are invariably associated with the propylitic assemblage, particularly with the leucoxene and, to a lesser extent chlorite. Where an assemblage of chlorite + leucoxene is pseudomorphous after biotite, most of the uranium is associated with the Ti-rich phase (Figure 12a). Where alteration has led to the growth of new hydrothermal chlorite, uranium may often reside within the chlorite itself (Figure 12b). Epidote is another alteration-related phase which acts as a host to low concentrations of uranium (Figure 12c). Sample V21 (Table 4), a strongly epidotized granite from the southern tip of the Westerdam dome (Figure 9), provides an example where U has been markedly enriched, with respect to Th, by concentration into epidote. Hematite (Figure 12d), as well as other Fe-oxyhydroxides, is another mineral phase which can concentrate significant quantities of uranium. The porphyritic granites of the Johannesburg dome, which have high U contents and low Th/U ratios, contain uranium hosted in hematite (Figure 12d), epidote and chlorite, as well as zircon, apatite, and monazite-like phases.

Higher concentrations of uranium are usually evident in granites that have been more severely altered by late-stage or vein-related alteration processes. Pegmatite veins often contain either uraninite or uranothorite. An example is provided by sample ST8 (587,5) from the hinterland to the Evander Goldfield, which is a pegmatite vein containing uranothorite and characterized by high U and Th contents (Table 4; Ferraz, 1989). Uraninite has also been observed in pegmatites from the Johannesburg dome (Hallbauer, 1982). The RAT1 borehole (Area 4B; Figure 9) intersected a suite of hydrothermally altered granites characterized by pervasive propylitic alteration, quartz-carbonate- chlorite-allanite-pyrite veining and fluorite-related micro-brecciation. These samples contain high U contents and typically have low Th/U ratios (0.3-2.5; Table 4), with uranium concentrated in moderate proportions within the propylitic assemblage (particularly leucoxene), and very strongly adsorbed around sulphide phases such as pyrite. Figure 13a shows an annular rim of pitchblende coating a rounded pyrite grain from sample RAT1 (1617). The RAT1 samples also contain small opaque uranium minerals which may be uraninite or coffinite, but have not yet been identified positively. The fact that fluorite is commonly observed in the RAT1 granites raises the possibility that uranium was transported as a halogenide complex (e.g. UF_5^-), a feature which may have been applicable to many uraniferous granites (e.g. Bushveld, French Massif Centrale, and Cornwall) where an association between uranium and fluorine is evident.

An interesting observation that has been made in the hydrothermally altered granites of the Witwatersrand Basin hinterland is the common occurrence of kerogen nodules (Hallbauer, 1984; Klemd and Hallbauer, 1987; Robb and Meyer, 1985). These nodules are particularly well developed in the peraluminous, greisenized granites northwest of the Klerksdorp Goldfield (Figure 9), but have also been observed along the Rand Anticline (Area 3, Figure 9), south of the Schweizer-Reneke dome (Area 7, Figure 9), and in the Welkom Goldfield hinterland (Area 8B, Figure 9). The kerogen nodules are hard, well-compacted, semi-anthracitic, hydrocarbon phases which consist of carbon (73-79%), hydrogen (2.8-3.1%) and oxygen (7.8-8.4%), and have H/C and O/C ratios that correspond to the catagenetic zone in the maturation of organic matter (P. Landais, pers. comm. 1987). They also invariably contain major concentrations of uranium (up to 7000 ppm in sample TKB (120)), are often gold-bearing (up to 900 ppb Au in sample TKB (120)) and are commonly associated with sulphides, in particular pyrite and chalcopyrite. Granites which contain kerogen nodules also have high U contents and will generally have low Th/U ratios. Examples are provided by samples TKB3 (120), GH1 (6137) and (6221), DHF9 (651), DSF11 (2625) and DRH10 (2825) where U contents range from 8.2-116.1 ppm and Th/U ratios from 3.7-0.15 (Table 4). The uranium that is associated with the kerogen nodules is not simply adsorbed into the margins of the nodules, but is patchily distributed throughout the hydrocarbon phase (Figure 13b). This suggests that the uranium actually exists as minute grains of uraninite within the kerogen, a feature which is well displayed in sample DHF9 (651) where a single large grain of uraninite is seen within a kerogen nodule which itself rims chalcopyrite (Figure 13d).

The origin of kerogen nodules in the hydrothermally altered granites is unknown at this stage. One explanation that has been provided is that they originate from within the Witwatersrand Basin itself and were transported *per descensum* into the basement by diagenetic fluids (Klemd and Hallbauer, 1987). A problem with this interpretation is that the kerogen nodules exist in granitoids which are not at present, and may never have been, overlain by Witwatersrand sediments. The kerogen also occurs in granites that exhibit different

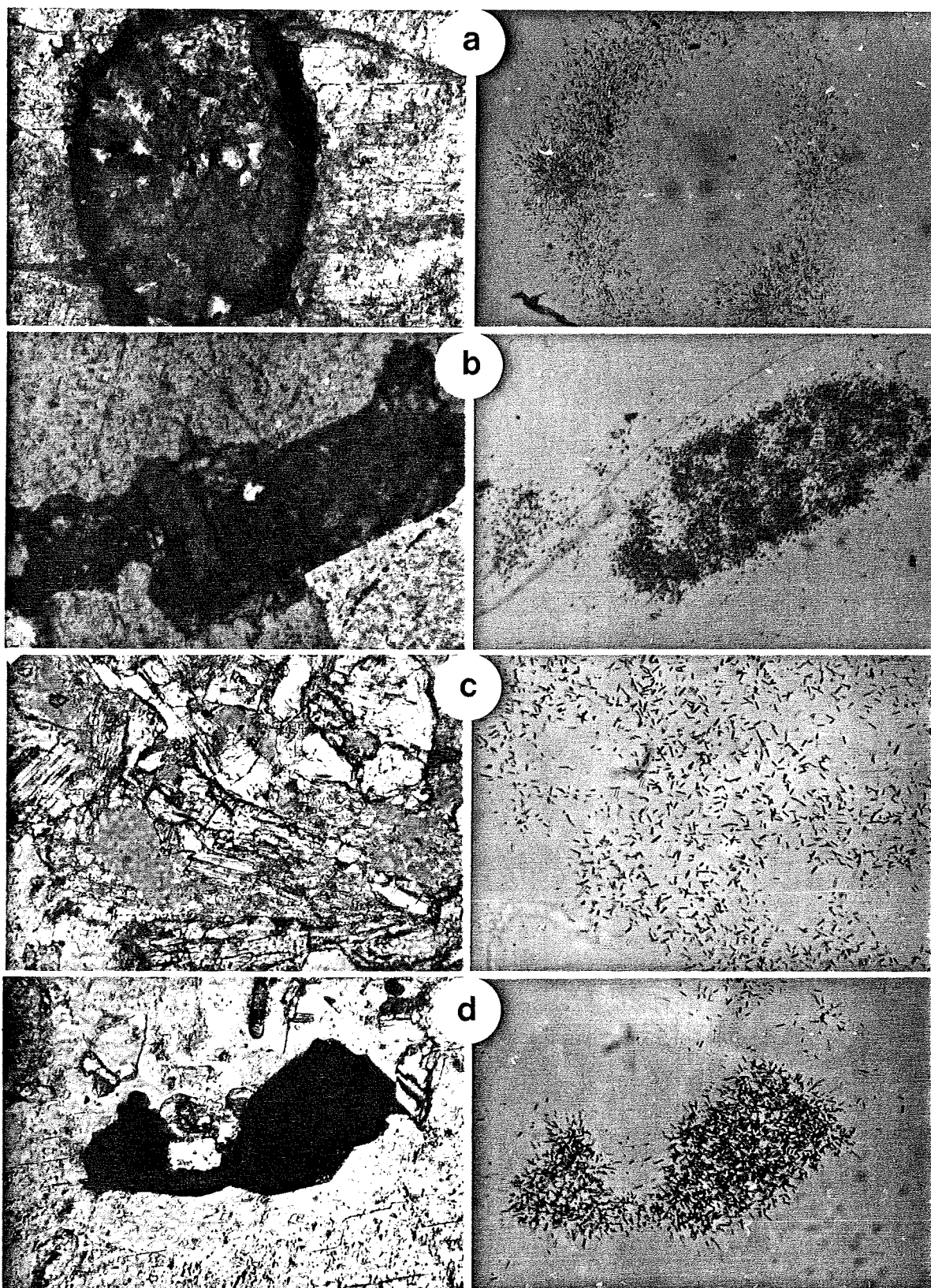


Figure 12 URANIUM DISTRIBUTION IN HYDROTHERMALLY ALTERED GRANITES FROM THE WITWATERSRAND HINTERLAND
a. Chlorite pseudomorph after biotite, rimmed by leucoxene, showing minor concentration of uranium into the latter.
b. Hydrothermal chlorite with corresponding fission track print showing concentration of uranium into this phase.
c. Coarsely crystalline epidote with corresponding fission track print showing uranium weakly concentrated into this phase. Field of view = 0,4 mm.
d. Small grain of colloform hematite and the associated distribution of uranium. Field of view = 0,4 mm.

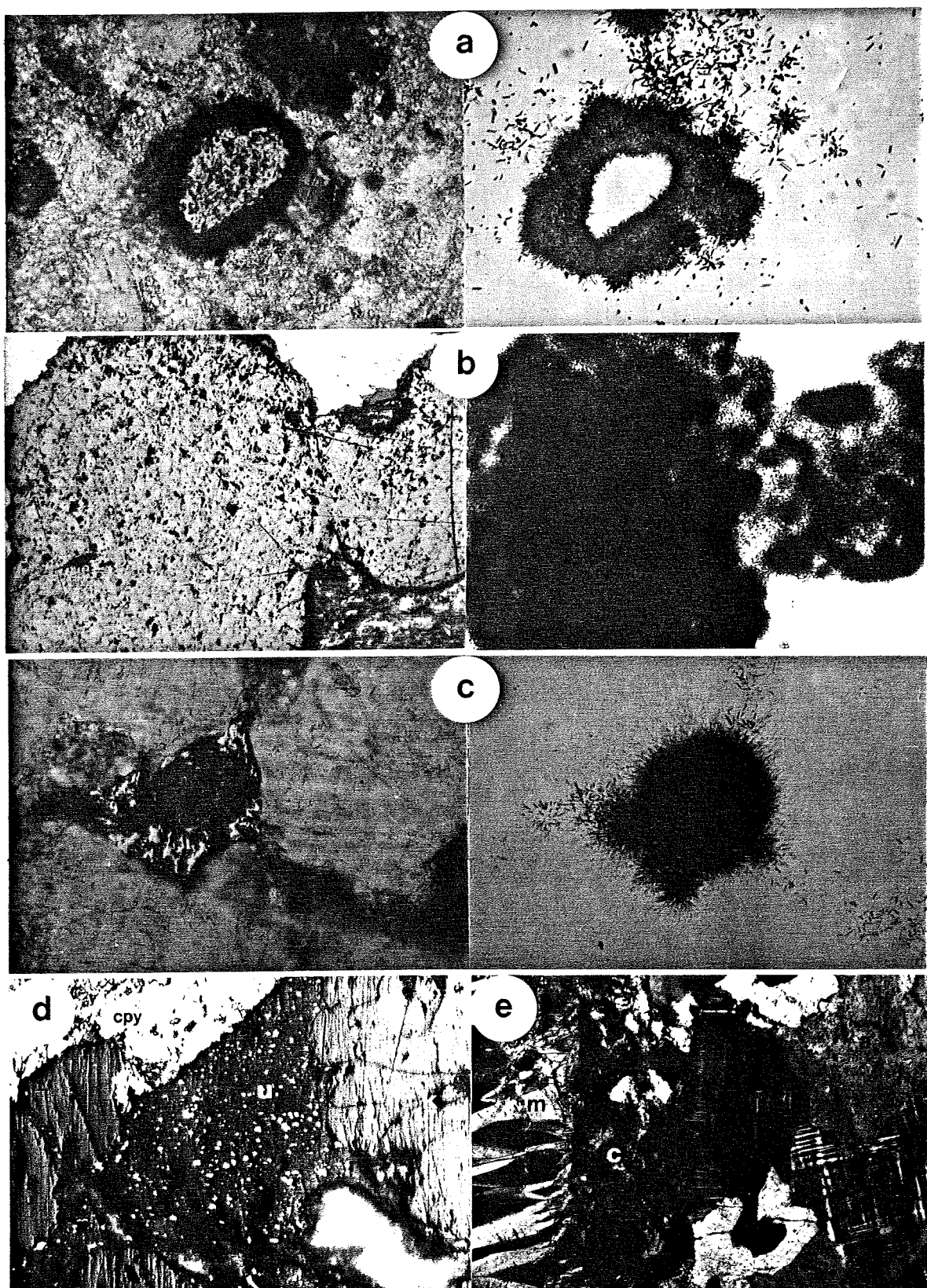


Figure 13 URANIUM DISTRIBUTION IN HYDROTHERMALLY ALTERED GRANITES FROM THE WITWATERSRAND HINTERLAND

- a. Rim of pitchblende coating pyrite in a hydrothermally altered granite.
- b. Large kerogen nodules; fission track micro-map shows high concentrations of uranium patchily distributed throughout the nodules.
- c. Small grain of uraninite associated with sulphides from a greisenized granite which is also characterized by low Th/U.
- d. Uraninite (u) and radiogenic galena (?) associated with kerogen (k) and chalcopyrite (cpy), from a greisenized granite. Field of view = 0,2 mm.
- e. Greisenized granite showing development of a muscovite fibre vein (m), chlorite (c) and albited microcline (a).

styles of alteration, not all of which could be attributed to diagenetic fluids. It is possible, therefore, that certain of the kerogen nodules, in particular those associated with the greisenized granites beneath the Dominion Group, may have an origin that is related to endogenous hydrothermal processes.

(i) Greisenized granites

Mention has been made above of the greisenized peraluminous granites in the area northwest of the Klerksdorp Goldfield. These granites do not have abnormally high U contents (maximum 24.1 ppm; Table 4), but are nevertheless characterized by low Th/U ratios, particularly when affected by greisenization. Because of the low Th contents, the common Th-bearing accessory minerals such as sphene, monazite, xenotime, and allanite do not occur within the greisens and even zircon and apatite occur infrequently. Consequently, even those granites with low U contents are able to crystallize uraninite, as uranium is not significantly appropriated by other low-solubility accessory phases (Cumey and Friedrich, 1987). An example of this is seen in sample DRH12 (1997) (Figure 13c) where uraninite represents the dominant host to uranium in the sample, and yet the total U content is only 4 ppm (Table 4). This sample is also, however, characterized by a very low Th/U ratio (0.65; Table 4), pervasive greisenization and albitization, and no Th-bearing accessory minerals, with the exception of rare zircon. Under these conditions, most of the uranium present in the rock is available for crystallization as uraninite.

Although in part a function of the original composition of the magma, the moderately high U contents, and the low Th/U ratios, that characterize the peraluminous granites northwest of Klerksdorp, are largely related to the hydrothermal alteration that has pervasively affected these rocks. Evidence for this is derived from the plot of Th/U versus Ce/Yb (Figure 14) where it is apparent that a correlation exists between the two ratios. Granites which have been markedly affected by pervasive greisenization have also suffered from severe depletion of the light rare earth elements (LREE), and are, therefore, characterized by low Ce/Yb ratios. The greisenized samples are also characterized by low Th/U ratios and it is clear, therefore, that alteration has resulted in collective mobilization of U-Th-LREE. This characteristic also pertains to the uranium-mineralized peraluminous granites of the French Massif Centrale (Cathelineau, 1987) where element mobilization has been attributed to the presence of saline hydrothermal solutions which are initially responsible for the dissolution of pre-existing accessory minerals such as monazite and xenotime, and the subsequent provision of Cl⁻ and PO₄³⁻ ligands for the transport of the LREE and U, respectively. Fluid inclusion studies on greisenized samples from the Klerksdorp area point to the presence of moderately saline (\approx 20 wt.% eNaCl) fluids that correspond to a composition within the H₂O-NaCl-CaCl₂ system (Robb 1987). No evidence is yet available, however, for the nature of the complexes responsible for the transport of uranium in the greisenized granites.

4. URANIUM IN PALAEOWEATHERING PROFILES ON THE ARCHAEOAN GRANITIC BASEMENT

The unconformity between basement rocks and overlying sedimentary or volcanic cover sequences in the Witwatersrand Basin hinterland is frequently characterized by a quartz-sericite alteration zone that is generally between 1-15 m wide. The lateral consistency of these alteration zones over wide areas beneath major unconformities has led to the suggestion that they represent palaeoweathering profiles (Button and Tyler, 1981; Robb and Meyer, 1985; Grandstaff *et al.*, 1986; Ferraz *et al.*, 1987) although it is also likely that they have been affected, to a varying degree, by diagenetic or metamorphic fluids moving along the unconformity (Holland and Zbinden, 1986; Palmer, 1987). Button and Tyler (1981) first emphasized the potential economic significance of these hiatuses and pointed out that the palaeoregoliths produced during early weathering processes, may have provided much of the bulk arenaceous detritus in depositories such as the Witwatersrand Basin. Furthermore, they also suggested that palaeosols may represent the sites where uranium was leached from the source area and transported, via ground water flow, into adjacent conglomeratic sediments. For this reason, as well as because of the generous availability of sample material, the U and Th distribution in these alteration profiles has been studied in order to complement the data that pertains to the primary source rocks.

A. Characteristics of Palaeoregolith Profiles

Palaeoregolith profiles are stratiform alteration zones with a sharp upper boundary which grades progressively into the parent granite. The profiles are normally zoned and comprise a bleached, yellow-green upper horizon which overlies a darker green lower section. The upper zone comprises mainly quartz and sericite together with minor aggregations and stringers of leucoxene (Figure 15a). In one particularly well-preserved profile obtained from borehole core which passed through the Black Reef quartzites into underlying granitic basement, the upper zone is characterized by ped-like features consisting almost entirely of sericite, and rimmed by leucoxene stringers (Ferraz, 1989). These features possibly indicate the preservation of a true fossilized soil or palaeosol which in most profiles is no longer preserved and only the regolith, or lower, less-altered portion remains.

The bleached palaeoregolith grades downwards into a yellow-green zone which contains chlorite in the matrix in addition to sericite and leucoxene. The latter mineral now occurs as discrete aggregates and may also be recognizably pseudomorphous after sphene, titanomagnetite, or biotite. This zone grades down into the granitic parent rock with K-feldspar becoming discernible and the primary rock texture becoming progressively apparent.

Significant variations in the major and trace elements occur through the palaeoregolith profiles and these have been studied by detailed sampling through the well-preserved pre-Black Reef sequence mentioned above (Figure 16). The most marked elemental variations occur in the upper portions of the palaeoregolith profile, whereas more consistent patterns, tending towards the parental composition, occur lower down. SiO₂ may be significantly enriched towards the top of the palaeosol, but depleted in areas where ped-like textures are preserved. Al₂O₃ and TiO₂ behave antipathetically to SiO₂ and reflect the increasing amounts of sericite and leucoxene in the palaeosol portion of the profile. Total iron is strongly depleted in the upper, bleached portion of the palaeoregolith but less so in the lower section where Fe⁺ may have been fixed by the development of chlorite. With regard to the alkali elements, Na₂O is consistently depleted in all portions of the palaeoregolith profile (Figure 16), as are CaO and Sr. K₂O is generally enriched in the palaeoregolith compared to the parent although the degree of enrichment varies considerably depending on the development of sericite.

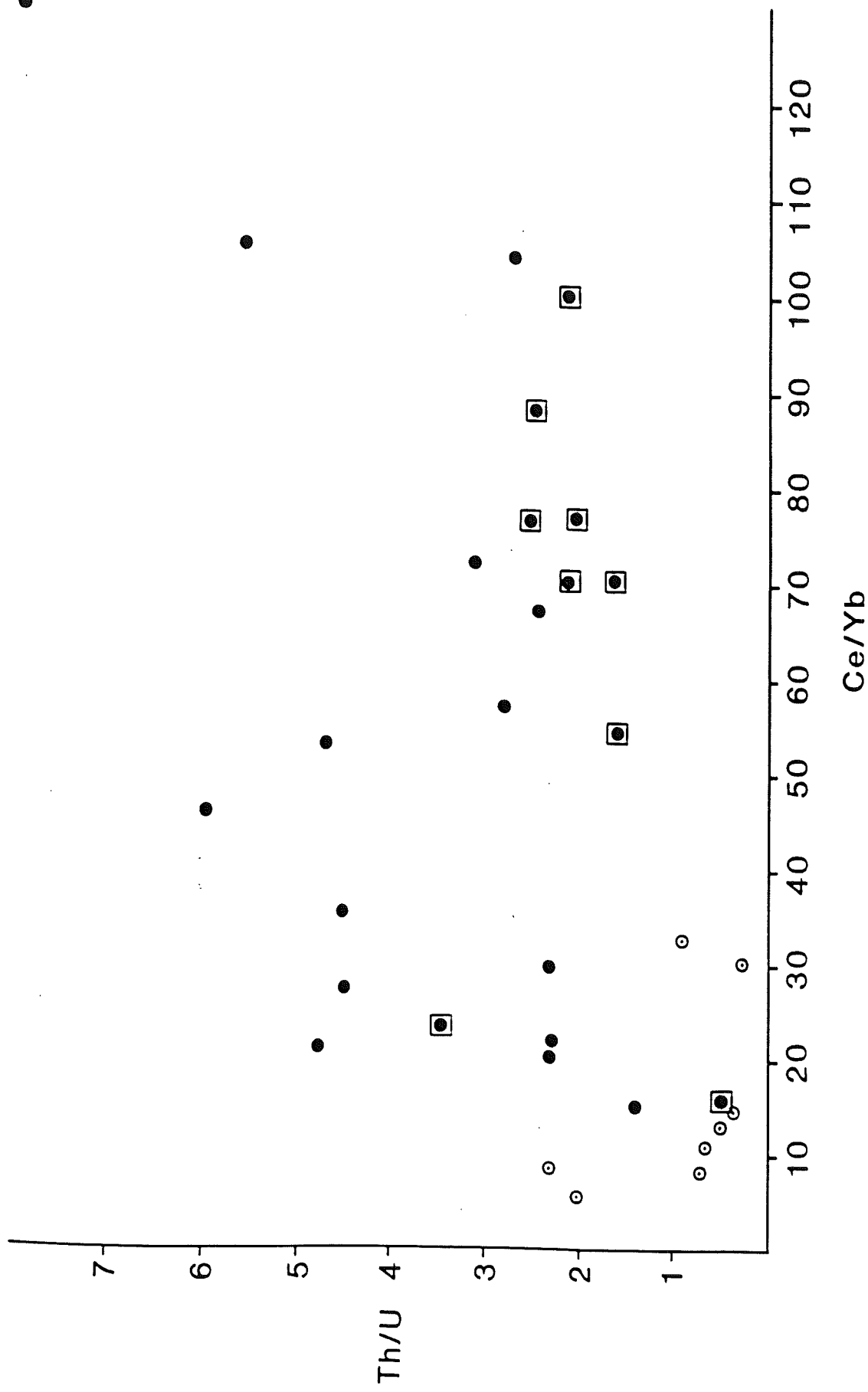
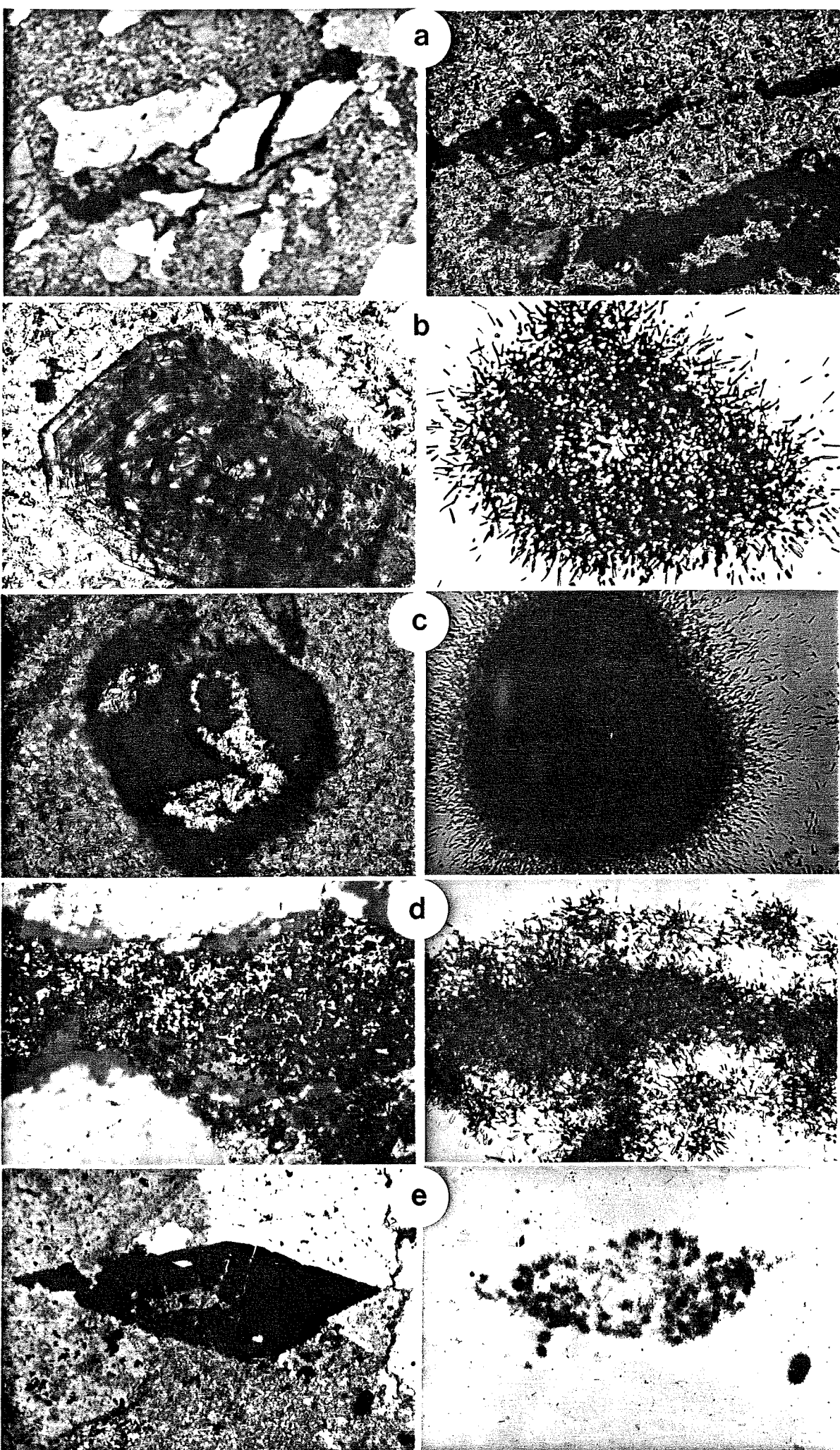


Figure 14: Plot of Th/U versus Ce/Yb for greisenized granites from area 5 (Figure 9). Severely greisenized samples (circle with dot) have low Th/U and low Ce/Yb (i.e. flat REE traces); albitized granites (boxed dots) also have low Th/U ratios but much higher Ce/Yb ratios.

Figure 15 URANIUM DISTRIBUTION IN PALAEOREGOLITH/ALTERATION PROFILES

- a. *Stringers and blebs of secondary leucoxene in the upper portion of the palaeoregolith profile.*
- b. *Secondary leucoxene showing an intimate association with small euhedral zircon grains thought to be authigenic in origin. Field of view = 0,4 mm.*
- c. *Zoned zircon, common to many of the palaeogoliths studied, showing a preferential concentration of uranium in the outer rim. Field of view = 0,4 mm.*
- d. *Unidentified urano-silicate phase (possibly coffinite ?) intimately associated with pyrite.*
- e. *Leucoxene (photographed in partial incident light) showing patchy uranium distribution.*
- f. *Leucoxene pseudomorph after sphene from the lower portion of a palaeoregolith profile.*



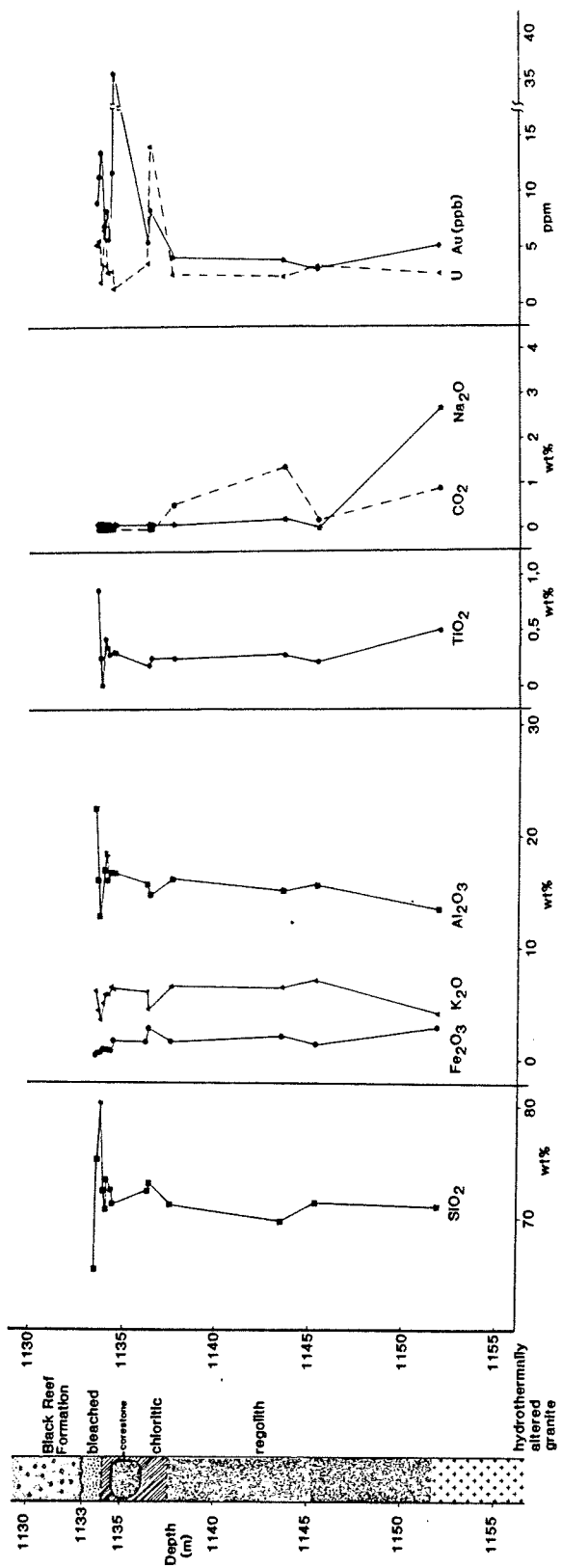


Figure 16: Schematic profile through a palaeoregolith section preserved beneath the Black Reef quartzite, as sampled in a borehole drilled in the Witwatersrand hinterland. Major and trace element variations along the profile are shown.

Au and U contents remain constant over much of the lower palaeoregolith profile, but show significant enrichment in the upper palaeosol portion. U enrichment is generally associated with the development of leucoxene stringers (see later), although a significant concentration of uranium also occurs at the base of the chloritic zone where an unidentified authigenic U phase may be developed (see later). Au is also enriched in certain portions of the palaeosol and, although its siting is uncertain, it is probably related to the development of authigenic sulphides particularly in the lower, chloritic portion of the profile. The volatile content (i.e. loss on ignition) of the palaeoregolith is invariably much higher than that of the parent rock and this reflects the development of abundant hydrous phases such as sericite and chlorite. The volatile species in the palaeoregolith are essentially aqueous, and a sharp depletion in $\text{F}^*\text{CO}_2 + \text{CO}_3$ is evident with respect to the parent (Figure 16). Quartz-calcite-sulphide veins which occur in the parent granite but not in the overlying palaeoregolith profile are, therefore, unlikely to represent the movement of late diagenetic fluids that may have altered the palaeoregolith profiles subsequent to their burial by overlying sediments.

B. Uranium and Thorium Distribution

A total of 50 samples, representing the palaeoregolith or alteration zone preserved beneath the basement unconformity in the Witwatersrand Basin hinterland, have been analysed in a U versus Th scattergram in Figure 17. It is clear from this plot that enrichment of U (i.e. >9 ppm) occurs in very few of the samples analysed and the maximum value recorded from the entire data set is 14.1 ppm. Furthermore, Th/U ratios do not deviate significantly from crustal values and there appears to have been little or no widespread leaching or concentration of uranium with respect to thorium.

Palaeoregolith samples have been collected from beneath three major basement unconformity surfaces, namely the pre-Dominion Group surface, the pre-Ventersdorp Group surface and the pre-Transvaal Sequence (i.e. Black Reef quartzite surface). There is no systematic difference in the U and Th contents of palaeoregoliths that can be ascribed to their formation at different periods in geological time. Pre-Ventersdorp palaeoregoliths in the present data set appear to have abnormally low radioelement abundances, but this can be attributed to the very low U and Th contents that characterize the parental tonalites and diorites over which the regolith was formed (Figure 17). Palaeoregoliths developed beneath the Dominion sediments also appear to be generally poor in uranium, a factor which may be partially due to their being largely underlain by the suite of greisenized granites described earlier, containing uranium which is hosted in easily leachable suites such as uraninite. Radioelement abundances in palaeoregoliths beneath the Black Reef quartzites are variable, with certain of the samples having high Th contents and/or high Th/U ratios (Figure 17). This may either reflect the primary composition of the parental granites or the fact that U was more prone to leaching by relatively oxygenated ground-waters in the early-Proterozoic, than it was previously.

The U versus Th plot in Figure 17 also illustrates the difference between radioelement contents in the palaeoregolith, and corresponding values for the respective parental granites, the latter obtained by averaging data in Table 4. In general, the observation by Button and Tyler (1981) that the palaeoregolith is depleted in uranium compared to the parental rock, is validated although in detail is somewhat oversimplified. Certain samples appear to be strongly depleted in Th but relatively conservative with respect to U, whereas others, although depleted in uranium, may even be slightly enriched in Th (Figure 17). This indicates that even the resistant Th-bearing accessory minerals in granites may be dissolved during pedogenesis or subsequent hydrothermal alteration, with Th being reconcentrated into suitable authigenically derived host minerals. A few palaeoregolith samples, or portions of palaeoregolith profiles (Figure 16) are, however, enriched either in uranium or both uranium and thorium. In these samples it is apparent that U and Th have been concentrated within a phase that formed during, or subsequent to, the formation of the palaeoregolith. This aspect is considered in more detail in the following section.

C. Uranium Distribution Evident from Fission Track Micro-mapping

Detailed fission-track micro-mapping studies reveal that uranium in palaeoregoliths is hosted either in small resistant accessory minerals that are inherited from the parent rock, or in authigenic phases that formed during the alteration processes.

The only resistant accessory mineral that occurs ubiquitously in the palaeoregoliths is zircon, although monazite has been detected in certain samples. The zircons are almost invariably zoned and contain prominent overgrowths which often contain significantly higher concentrations of uranium than the cores (Figures 15b). The zoned aspect, which is commonly associated with zircons in palaeoregoliths suggests that the overgrowths may be authigenic in origin, forming either during alteration or pedogenesis. This view is supported by the observation, in one palaeoregolith profile, of small, euhedral, authigenic zircon crystals intimately associated with the leucoxene stringers which are otherwise ubiquitous in these rocks (Figure 15a,b). The concentration of uranium into authigenic zircon grains and overgrowths represents one mechanism whereby uranium may be fixed in the palaeoregolith.

A significant proportion of uranium in the palaeoregoliths (as evident from the distribution of fission tracks) is also concentrated into opaque phases which are authigenic in nature. Samples with high radioelement contents (e.g. BSP10(III); Table 5) exhibit a preferential concentration of U into opaque amorphous, spongy phases which may be coffinite, but which can probably best be described non-definitely as "pseudogummite" (Figure 15d). In samples with lower radioelement contents, fission track prints clearly illustrate that most of the uranium resides in the ubiquitous leucoxene blebs and stringers that occur throughout the alteration profile (Figure 15e). In the lowermost sections leucoxene is generally pseudomorphic after a pre-existing Ti-bearing phase such as sphene (Figure 15f), titanomagnetite or biotite. The uranium content, evident in terms of relative fission track densities, in the pseudomorphic leucoxene is generally low and probably does not greatly exceed that in the original material. In the upper section of the palaeoregolith profile, stringers and aggregates of authigenic leucoxene and rutile occur (Figure 15a), and these may contain high concentrations (100-1000 ppm) of uranium (Figure 15e). The concentration of uranium into Ti-rich phases reflects the well-known geochemical affinity between U^{4+} and Ti^{4+} , a feature which results in the fact that many of the uranium-bearing multiple-oxide group of minerals (e.g. davidite, betafite, brannerite, etc.) have Ti as a stoichiometric constituent. It appears, therefore, that the palaeoregoliths not only represent sites in the Witwatersrand hinterland where uranium was leached from the source rocks (Button

TABLE 5

**U and Th Contents of Palaeoregolith Profiles in the Hinterland
of the Witwatersrand Basin**

	Th	U		Th	U
AREA 2 (BR)			KK3	28,90	7,55
			KK4	32,20	5,60
VOK1 (8586)	24,00	2,55			
VOK1 (8592)	15,00	1,68	(VD)		
VOK1 (8594)	11,30	1,22	LLP2 (804)	20,10	1,04
SA1 (206,2)	12,80	1,82	LLP2 (807)	2,97	0,62
SA1 (206,5)	24,00	2,23			
ZT1 (8671)	13,90	2,01	AREA 4A (DOM)		
ZT1 (8676)	44,00	1,80	BWP1 (116)	26,40	9,79
KN1 (5199)	11,00	2,92	BPF1 (140,1)	14,70	3,77
BH155 (3718,6)	10,20	5,54	BSF1 (757)	17,40	3,53
BH155 (3718,9)	11,00	5,71	BBS3 (325,2)	5,34	1,46
BH155 (3719,1)	8,87	2,06			
BH155 (3719,8)	18,90	6,67			
BH155 (3720,2)	10,50	3,49	AREA 5 (DOM)		
BH155 (3720,6)	11,60	2,88	DOF1 (564)	9,79	4,26
BH155 (3721,0)	12,90	2,98	DOF1 (566)	10,70	4,26
BH155 (3721,6)	4,09	1,51	DRH8 (1469)	15,10	2,11
BH155 (3727,6)	10,70	3,66	DRH8 (1484)	10,70	0,56
BH155 (3728,0)	9,63	14,10	DRH12 (1948)	6,56	1,45
BH155 (3732,0)	8,98	2,65	DSF7 (3617)	3,47	1,45
BH155 (3752,0)	10,20	2,53	SF5 (79,8)	9,94	2,63
BH155 (3758,0)	9,00	3,38			
AREA 3 (BR)			AREA 7 (DOM)		
BSP8 (iii)	27,90	8,48	VF12 (812,3)	12,50	1,85
BVK4 (90)	35,80	5,84	VF12 (817)	8,47	1,05
BKK8 (104)	18,60	4,56			
R1	89,00	11,90	AREA 7 (VD)		
R2	10,70	3,91	TA1 (468)	4,02	0,65
R3	15,30	3,48	TA1 (470,7)	4,63	0,19
KK1	2,47	0,74	TA2 (330)	4,33	0,63

Note (i) Area localities outlined in Fig.9

(ii) Palaeoregolith profiles underlie:- Black Reef (BR)
Dominion Reef (DOM)
Ventersdorp Supergroup (VD)

and Tyler, 1981), but also reflect zones where uranium, transported either colloidally or in solution, was actively deposited and, in some instances, concentrated. The significance of U-Ti phases in the palaeoregolith insofar as the origin of brannerite in the Witwatersrand Basin is concerned, is discussed later.

5. SOME ASPECTS OF THE URANIUM DISTRIBUTION IN WITWATERSRAND REEFS

The nature and occurrence of uranium mineralization in the Witwatersrand reefs is now reasonably well understood, having been the object of many detailed studies over the past three decades (Liebenberg, 1955; Hiemstra, 1968; Ramdohr, 1958; Schidlowski, 1966; Feather, 1981; Hallbauer, 1981; Smits, 1984 and many others). Uranium mineralization occurs in essentially three modes:

- (1) as detrital components of which uraninite is the most important. Other uranium-bearing detrital phases include zircon and monazite;
- (2) as complex U-Ti phases which range in composition from uraniferous leucoxene to brannerite. Most of these phases are believed to have formed authigenically, although it is generally accepted that a detrital precursor phase must have been involved in their formation; and
- (3) in association with carbonaceous matter which occurs, either in the form of polymerized hydrocarbons and seam-like kerogen which is intimately associated with uraninite, or as granular "fly-speck" kerogen nodules.

The nature of the uranium mineralization in the Witwatersrand Basin is both complex and diverse and involves, not only the introduction of detrital uraninite, but also the epigenetic reconstitution of labile uranium. These processes cannot be fully understood without recourse to the distribution of uranium, and mechanisms of its preconcentration, in the source area of the basin.

A. Source Area Considerations

Many of the reef horizons in the Witwatersrand Basin are characterized by a correlation between Au and U, although considerable variation exists in the relative abundance of the two elements. This has been attributed to mechanical sorting of gold particles and uraninite during the formation of the sedimentary placer (Smith and Minter, 1980). However, the differing specific gravities of uraninite and gold result in a decrease in the Au/U ratio down the palaeoslope and, consequently, curvilinear regression curves result when Au and U distribution data are plotted on arithmetic coordinates (Smith and Minter, 1980). When the same data are plotted using logarithmic coordinates, however, linear regression curves, with the form $\log \text{Au} = m \cdot \log \text{U} + c$ result (Smith and Minter, 1980; Robb and Meyer, 1985). When data from a number of reef horizons are regressed and compared, the different slopes and intercepts that result provide a means of evaluating Au and U distribution as a function of sedimentological sorting and source control. If any two reef horizons are compared in which sedimentological parameters are similar, then observed differences can probably be attributed almost entirely to the nature of the source (Smith and Minter, 1988).

In Figure 18 curves for Au and U distribution data for a number of different reef horizons are plotted, and reveal differing slopes and intercepts on both coordinates. In general it is apparent that U contents in the reefs are between one and two orders of magnitude greater than the Au contents. It is also evident in Figure 18 that most of the Witwatersrand reefs (e.g. Vaal, White) are characterized by 45° slopes indicating that a factor increase in U is matched by a similar factor increase in Au (i.e. an order of magnitude increase in Au is accompanied by an order of magnitude increase in U). This indicates that the abundance of uranium is far greater than that of gold in the source rocks from which the sediments were derived if both elements were introduced as particulate detritus. This reasoning also applies if gold and uranium have been conservatively remobilized *in situ*, but may not be relevant if the two elements were introduced in solution into the basin.

Certain of the Au-U curves in Figure 18 have slopes which deviate significantly from 45°. In such cases the factor increase in Au may be greater than that for U, or *vice versa* (e.g. Elsburg and Promise Reefs, Figure 18). In such instances, the source rocks providing detritus into the depository may have been more specifically enriched in the one element than in the other. This may be the case where the source was dominated by uranium-deficient greenstone belts containing Au-quartz lodes, on the one hand, or a suite of uranium-rich granites with a few contained greenstone remnants, on the other. Certain curves, or sets of curves, may have similar slopes but are laterally transposed with respect to one another (Figure 19), indicating an overall enrichment in the one element for any corresponding value of the other element. This is the case when comparing the Kimberley Reef in the Evander Goldfield, with the same reef in the East Rand Goldfield. In this case it is clear that for any value of Au, uranium is consistently more enriched in the East Rand than in the Evander Goldfield (Figure 19). Such differences have been attributed to fundamental differences in the nature of the Archaean basement in the source areas of the two regions (Ferraz, 1989). Au-U distribution curves, as well as other parameters such as zircon/chromite ratios, pebble populations, and total PGE contents, may, therefore, be instructive in assessing the nature of the source area to any particular reef horizon.

B. Uranium and Thorium Distribution in Witwatersrand Reefs

(i) The Promise Formation, Government Subgroup, West Rand Group

The Promise Formation consists of numerous, stacked, small-pebble conglomerates occurring at the base of a number of upward-fining arenite sequences interpreted as a series of coalesced fan-deltas prograding onto a marine shelf (Meyer and Tainton, 1986). The detrital ore minerals which occur within the Promise Reefs in the Klerksdorp and West Rand areas include pyrite, zircon, chromite, monazite, ilmenite, arsenopyrite, cobaltite, rutile, kerogen nodules, thorite, allanite, uraninite, and gold. Authigenic minerals include pyrite, chalcopyrite, pyrrhotite, leucoxene, brannerite, and many other sulphide phases (Meyer and Tainton, 1986). The most abundant detrital phases are pyrite, zircon, chromite and, to a lesser extent, monazite. Thorite was observed in a few samples and uraninite is extremely rare.

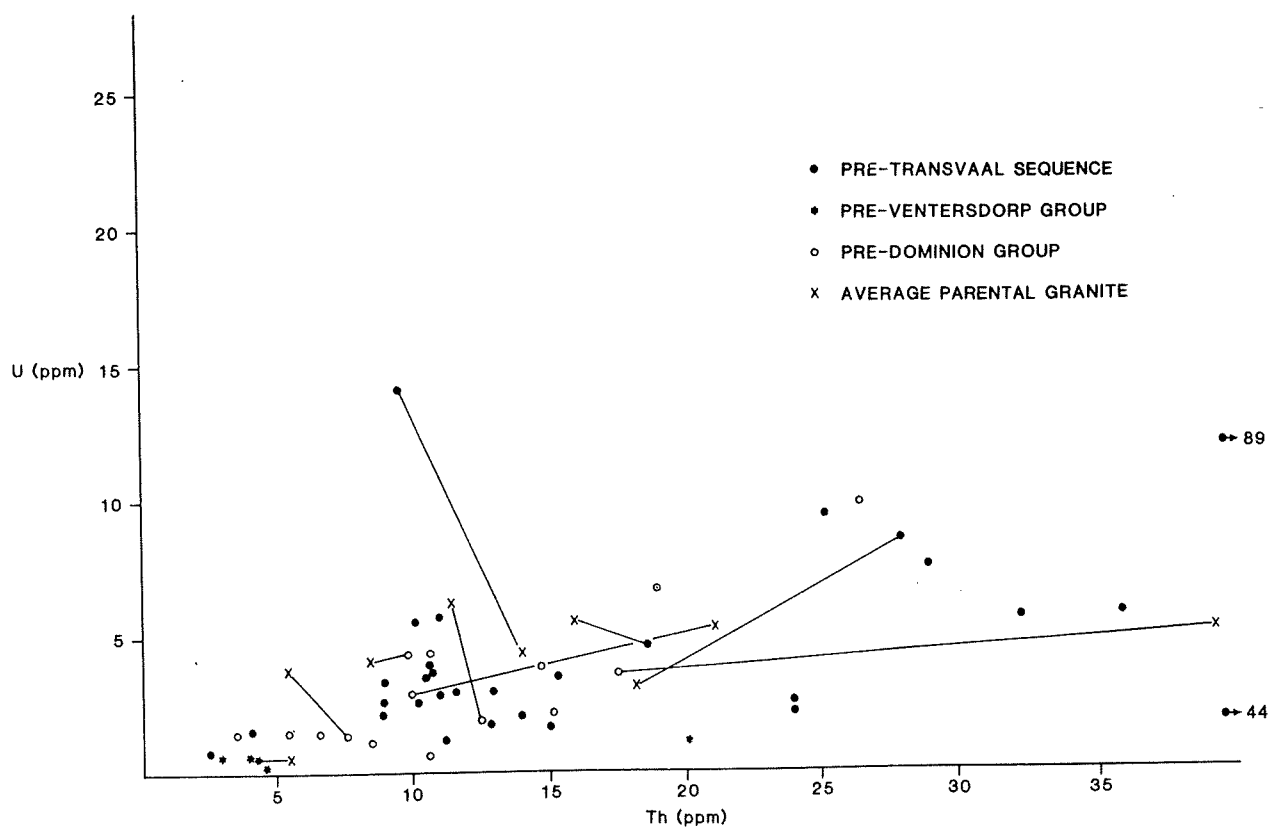


Figure 17: Plot of U versus Th for palaeoregolith samples preserved beneath the Transvaal Sequence and Ventersdorp and Dominion Groups. Where available the average uranium and thorium contents of the parental granite from which the regolith was derived are plotted (see tie-line points).

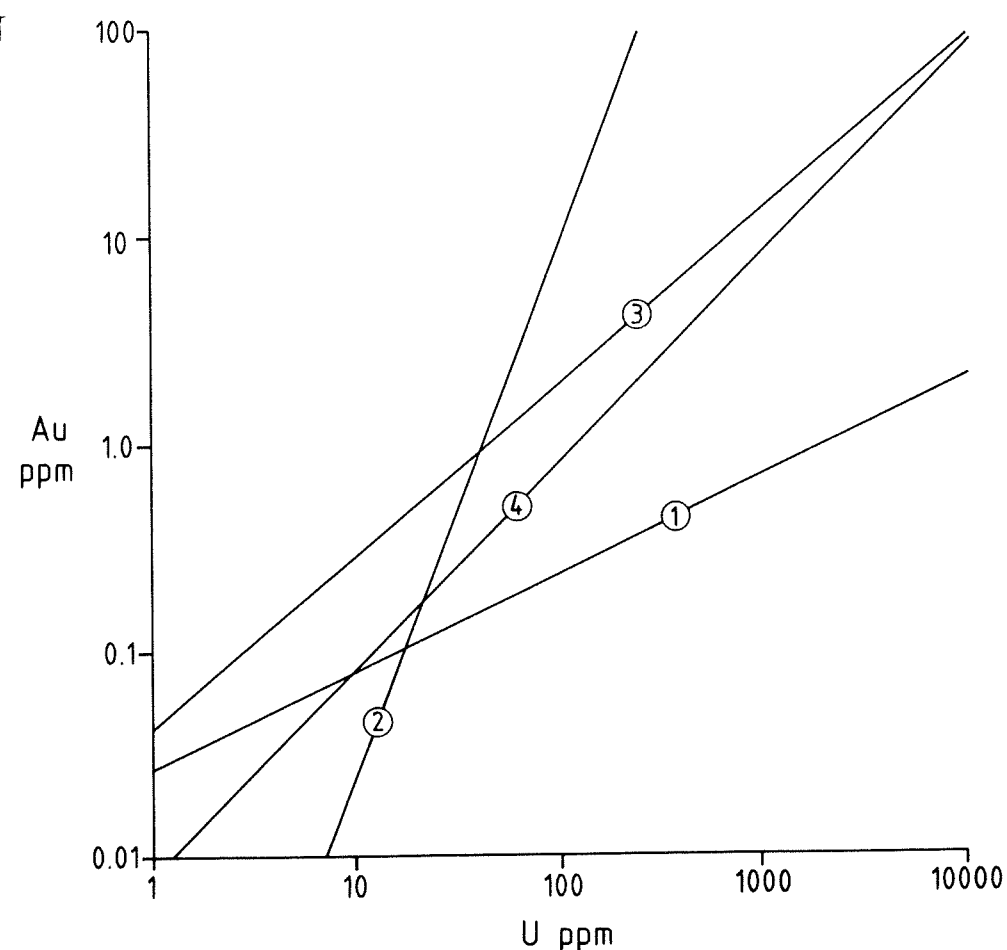


Figure 18: Plot of Au versus U for certain selected reef horizons in the Witwatersrand Basin showing the extent to which the slopes of best-fit curves can vary. Ranges of Au and U are deliberately not shown and curves are extrapolated to intersect co-ordinates. 1 = Promise Reefs; 2 = Elsburg Reef; 3 = Vaal Reef; 4 = White Reef. Data from Robb and Meyer (1985).

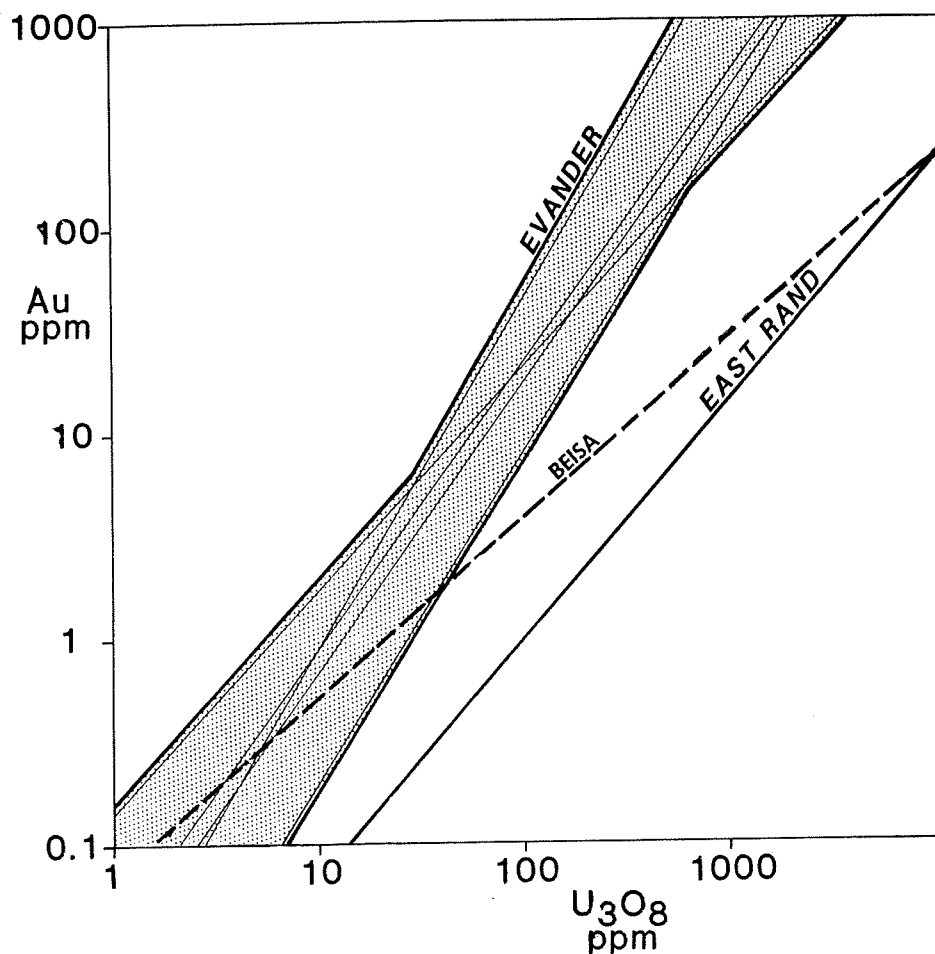


Figure 19: Plot of Au versus U for the Kimberley Reef from the Evander and East Rand Goldfields. Also shown is data for the Beisa Reef from the Welkom Goldfield. Data are from Ferraz (1989) and Drennan (1988).

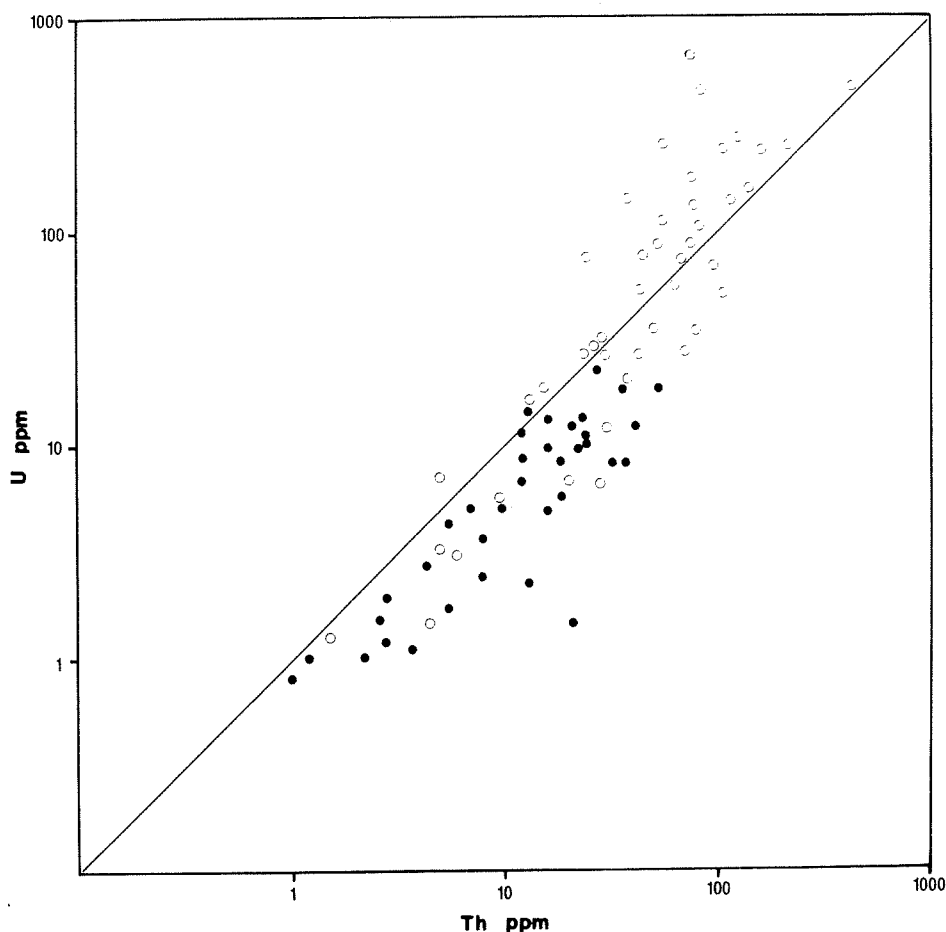


Figure 20: Plot of U versus Th for samples from the Promise Reefs showing values for conglomerate bands (open circles) and intercalated footwall and hanging wall quartzites (dots). Data from Meyer and Tainton (in prep.).

Uranium values in the Promise Reefs vary from 1-630 ppm with gold varying from 0,1 to 30 ppm. The Au-U curve in Figure 18 has a relatively flat slope implying that the source rocks from which detritus was derived were far more U-specific than Au-specific. In spite of this the Th/U ratio is comparatively high (\approx 0,5) which is a reflection of the abundance of minerals such as monazite and thorite.

Thirty-six samples of the Promise conglomerates, as well as a number of quartzites adjacent to the conglomerates, were analysed for their U and Th contents and the results plotted in Figure 20. The quartzites clearly have much lower radioelement contents than the conglomerates, and also have different Th/U ratios. The quartzites plot beneath the $U = Th$ line in Figure 20 and have Th in excess of U, whereas many of the conglomerates are the converse, with U greater than Th. This is primarily due to the preferential development of authigenic uranium-bearing phases, such as uraniferous leucoxene and brannerite, in the conglomeratic horizons. There may be two reasons for this, firstly because of the preferential accumulation of uranium-bearing heavy minerals together with other coarse detritus in the conglomerates and, secondly, because of the greater porosity of the conglomerates which facilitates the movement of fluids and the development of authigenic mineral phases capable of concentrating uranium in preference to thorium.

Mineralogical and geochemical data indicate that the suite of heavy minerals in the Promise Reefs – and indeed in the lower portions of the Witwatersrand Supergroup in general – is more akin to that in the Dominion Group and Pongola Supergroup conglomerates, than to the assemblages characteristic of the Central Rand Group (Meyer and Tainton, 1986). These differences are particularly evident when considering thorium-bearing minerals such as monazite and thorite which are relatively abundant in the older successions, but relatively rare in overlying accumulations.

(ii) The Beisa Reef, Virginia Formation, Central Rand Group

The Beisa Reef occurs at the base of the Virginia Formation in the Welkom Goldfield and is anomalously enriched in uranium, but contains uneconomic concentrations of gold. The uranium mineralization is closely associated with abundant kerogen, particularly in the more distal reef facies. The kerogen seams, which are often multiply stacked within a single 30 cm thick section of reef, contain abundant inclusions of quartz, zircon, and uraninite, the latter occurring as well-rounded grains that are generally compact, but which may also be fragmented by the kerogen. Secondary kerogen, which possibly represents a light, migrated hydrocarbon fraction, occurs as veinlets cross-cutting the older kerogen seams and is generally uranium-deficient. Most of the pyrite in the Beisa Reef is rounded and compact, but also occurs as remobilized stringers and veinlets, together with leucoxene and galena (Drennan, 1988).

A plot of Au versus U_{38} for the Beisa Reef (Figure 20) reveals a relatively shallow best-fit curve which reflects the paucity of gold and anomalous enrichment of uranium. This form of Au-U distribution pattern possibly indicates that the source of Beisa Reef detritus was essentially uranium-specific and probably granitic (*sensu lato*). A similar scenario probably applies to the source area of the Promise Reefs in the Klerksdorp and West Rand areas, although in the case of the Beisa Reef the uranium contents are much higher.

(iii) The Kimberley Reef in the East Rand and Evander Goldfields

The Kimberley Reef has been mined for gold and uranium in the East Rand Goldfield, whereas further east in the Evander Goldfield it is exploited only for gold and is generally uranium-poor. Sediment-supply directions indicate that the source areas of the Kimberley Reef in the two goldfield areas are quite different (Figure 9), suggesting that broad differences in the nature of the source rocks may have played a role in affecting the regional characteristics of the Kimberley Reef (Ferraz *et al.*, 1986).

The Kimberley Reef at Evander is characterized by a more heterogeneous, polymictic pebble assemblage and a significantly higher average chromite/zircon ratio than the Kimberley Reef in the East Rand. The total platinum group element (PGE) content of the Evander Kimberley Reef is also markedly higher (i.e. = 90 ppb) than the same reef in the East Rand (= 4 ppb), and is also anomalously enriched with respect to the Witwatersrand average of approximately 12 ppb (Pretorius, 1976). These factors suggest that the source rocks to the Kimberley Reef at Evander comprised a significant component of mafic/ultramafic greenstone remnants capable of providing a diverse pebble population and the anomalously high chromite and PGE contents observed (Ferraz *et al.*, 1986). Such a suggestion is further supported by a consideration of Au versus U_{38} distribution data for the two areas (Figure 20). It is apparent when comparing regression curves, that the Kimberley Reef in the East Rand contains significantly more uranium than the Kimberley Reef at Evander. Thus, the source rocks supplying detritus to the Kimberley Reef at Evander were essentially gold specific and, therefore, inherently different to the rocks supplying detritus to reefs such as Promise and Beisa. This accords with the observed nature of the Evander hinterland which is underlain largely by granitoids of tonalitic and granodioritic composition – which are themselves generally uranium-poor (see Figure 2 and 3) – as well as numerous greenstone remnants (Ferraz *et al.*, 1986). Source rocks to the Kimberley Reef in the East Rand contain a great proportion of potassiac granitoids, some of which exhibit intense hydrothermal alteration and veining (Ferraz *et al.*, 1986), and also contain far fewer preserved greenstone remnants. Reef characteristics on a regional scale clearly, therefore, reflect the nature of the respective source rocks in the hinterland.

C. Comparative Mineralogy of Conglomerates on the Kaapvaal Craton

Conglomerates occur in a number of the Archaean to early Proterozoic sedimentary units on the Kaapvaal Craton including, in chronostratigraphic order, the Moodies Group, Pongola Supergroup, Dominion Group, Uitkyk Formation, as well as the West Rand and Central Rand Groups. Conglomerates within these various successions generally contain only minor concentrations of gold and uranium, with the marked exception of the Central Rand Group sequences with their enormous economically exploitable accumulations of Au and U. It would appear, therefore, that the hinterland region was markedly enriched with respect to both Au and U specifically during deposition of the upper Witwatersrand sediments and that this condition prevailed neither before, nor after, Central Rand Group times.

The anomalous characteristics of the upper Witwatersrand conglomerates can also be emphasized in terms of their uranium-thorium mineralogy, as shown in Figure 21. It is apparent that conglomerates from the upper Witwatersrand succession contain the highest relative abundance of phases such as uraninite, brannerite,

and fly-speck carbon, but a relative paucity of minerals such as monazite and thorite. By comparison, conglomerates from the lower Witwatersrand and Dominion successions - which occupy the same depositary - contain abundant monazite and thorite, but do not exhibit the same degree of uraninite concentration. Consequently, much of the source region to Central Rand Group sediments must have been enriched, not only in gold, but in uranium too. The mineralogical differences between Central Rand and pre-Central Rand Group conglomerates are also emphasized in the U/Th ratio plot in Figure 21. The older conglomerates have fairly low U/Th ratios (1-3) whereas the upper Witwatersrand conglomerates have, on average, much higher U/Th ratios (8-9) which reflect the higher concentrations of uraninite and brannerite. In general, therefore, source rocks to the upper Witwatersrand sediments appear to have been enriched in uranium, not only in absolute terms, but also with respect to thorium.

6. THE SOURCE OF URANIUM IN THE WITWATERSRAND BASIN

Over the past 35 years in excess of 150 000 tons of U_3O_8 have been produced from 31 mines in the Witwatersrand Basin (Pretorius, 1986). Although slightly less than half of this production was derived from one area (the Klerksdorp Goldfield, Figure 9), uranium occurs in economically exploitable concentrations as a by-product of gold mining over most of the basin, with only the Evander region being notably depleted in the commodity. It follows that the Witwatersrand hinterland as a whole must have been capable of providing enormous quantities of uranium into the depository, much of which was in the form of uraninite. Although the source of this uraninite is itself intriguing, a more perplexing problem relates to the fact that uranium was concentrated in the reefs without there having been a concomitant enrichment of thorium and/or thorium-bearing accessory minerals. The following section summarizes the presently available data pertaining to the regional, lithological and secular distribution of uranium in the Archaean granitic basement of the southern Kaapvaal Craton and attempts to provide a framework within which the problems concerning the source of Witwatersrand uranium may be addressed.

The detrital origin of much of the uraninite in the Dominion and Witwatersrand conglomerates is confirmed by their rounded or muffin-shaped outlines - attributable to abrasion (Liebenberg, 1955; Ramdohr, 1958; Schidlowksi, 1966, etc.) - as well as to the old U-Pb ages (> 3.0 Ga) obtained from uraninite separates (Niclaysen *et al.*, 1962). By contrast, however, considerable evidence also exists for the presence of labile uranium, which is required in the formation of authigenic phases such as leucoxene and brannerite. Consequently, any considerations regarding the origin of uranium in the Witwatersrand Basin needs to accommodate both a detrital origin for particulate uraninite and a source of labile uranium for the formation of authigenic phases.

Studies of U and Th distribution in granitoids of the Barberton Mountain Land indicate that radioelement abundances are dependent on rock type and age. Uranium and thorium contents increase progressively from the tonalite-trondhjemite gneisses of the First Magmatic Cycle, to the highly differentiated granites of the Third Magmatic Cycle. The causes of this secular enrichment process are complex and include progressive reworking (anatexis) of pre-existing crust, the nature of the granitic source rocks, the level of intrusion in the crust, and petrological factors such as crustal fractionation and the evolution of volatile phases. In addition, it is suggested that the peak of radioelement concentrations that appears to exist in the late granites of between 2.8-2.7 Ga old in the Barberton Mountain Land may be genetically linked to a widespread event of granulite facies metamorphism and uranium-thorium depletion of the lower crust at a similar time (Hart *et al.*, 1981; Slawson *et al.*, 1976). These concepts are schematically illustrated in Figure 22A, where it is inferred that uranium and thorium were systematically concentrated into high-level, differentiated granitoids by fundamental crust-forming events, at a time which somewhat preceded the development of, at least the upper portion, of the Witwatersrand sediments.

Many of the granites which were intruded into the Archaean basement of the Witwatersrand hinterland preserve evidence of hydrothermal alteration, a process which is attributed either to the evolution of volatile phases from within the granite itself, or to convection of meteoric fluids associated with the intrusion of the body (Robb and Meyer, 1986). These hydrothermally altered granites also provide evidence for the remobilization of uranium, and it is clear that uranium is decoupled from thorium and preferentially concentrated into suitable alteration assemblages within the granites. Of particular relevance are the low-Ca granitoids which, in the Barberton Mountain Land, are characterized by low Th/U ratios and relatively high U contents. In addition the greisenized peraluminous granites northwest of the Klerksdorp Goldfield are also characterized by low Th/U ratios and uranium that is commonly hosted in uraninite. Hydrothermally altered granites, therefore, point to the fact that uranium has been pre-concentrated in some of the source rocks of the Witwatersrand sediments and, in certain instances, decoupled from thorium to the extent that uraninite forms the predominant host-mineral in the source environment (Figure 22B). This is highly pertinent to the observation that upper Witwatersrand reefs contain detrital uraninite as the principal uranium-bearing phase, and have few, if any, phases containing thorium.

In the present study, attention has been drawn to the fact that the Witwatersrand hinterland also contains the preserved remnants of laterally extensive alteration zones which may be the vestiges of weathering profiles over the Archaean basement. Such zones, which may also have been somewhat modified by post-burial alteration processes, are the logical sites from which labile uranium could have been derived (Figure 22C). Soil-forming processes occur over a time span of 10^5 - 10^6 years and it is, therefore, likely that the source rocks to a sedimentary deposit that formed over a period of 10^7 - 10^8 years will undergo extensive weathering and pedogenesis. It is evident that uranium has been depleted from certain portions of the palaeoregolith profiles studied, and this could, therefore, represent a source of labile uranium, as suggested by Button and Tyler (1981). It is also apparent, however, that the palaeoregolith profiles contain ubiquitous leucoxene which was derived from the breakdown of titanium-bearing phases such as titanomagnetite, ilmenite, biotite, and hornblende. This leucoxene is compositionally variable and consists predominantly of Ti, moderate to minor quantities of Fe, Ca, Si, and Al, and uranium. The formation of uranium-bearing leucoxene in the palaeoregolith (Figure 22C) can possibly be regarded as a precursor to the "Pronto" reaction (Ramdohr, 1958) which occurs within the depository itself, where it is envisaged that U and Ti are reconstituted during diagenesis and/or metamorphism of the sediments to form authigenic brannerite (UTi_2O_6) and uraniferous leucoxene. The role of weathering in the source rocks to the Witwatersrand sediments has largely been over-looked in ore-genetic considerations and yet may provide answers to many of the enigmas that still

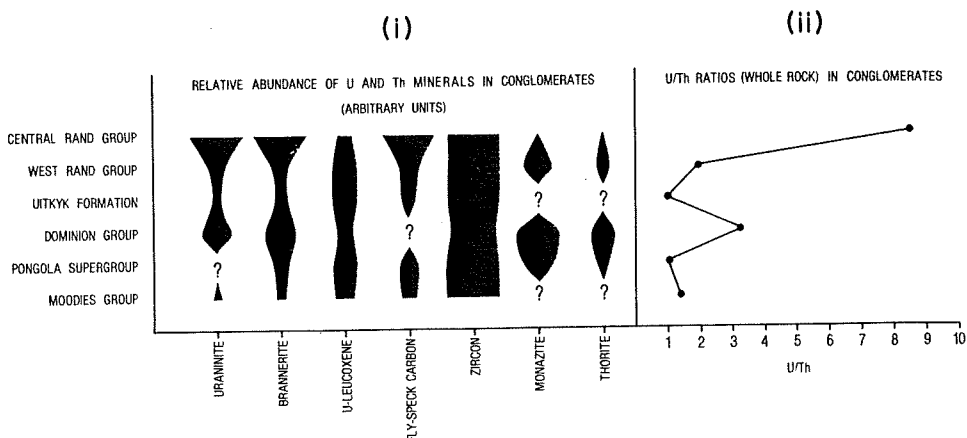


Figure 21: (i) Relative abundances of uranium and thorium minerals in conglomerates from the Kaapvaal Craton and, (ii) variation of whole rock U/Th ratios in the same conglomerates (from Robb and Meyer, 1985).

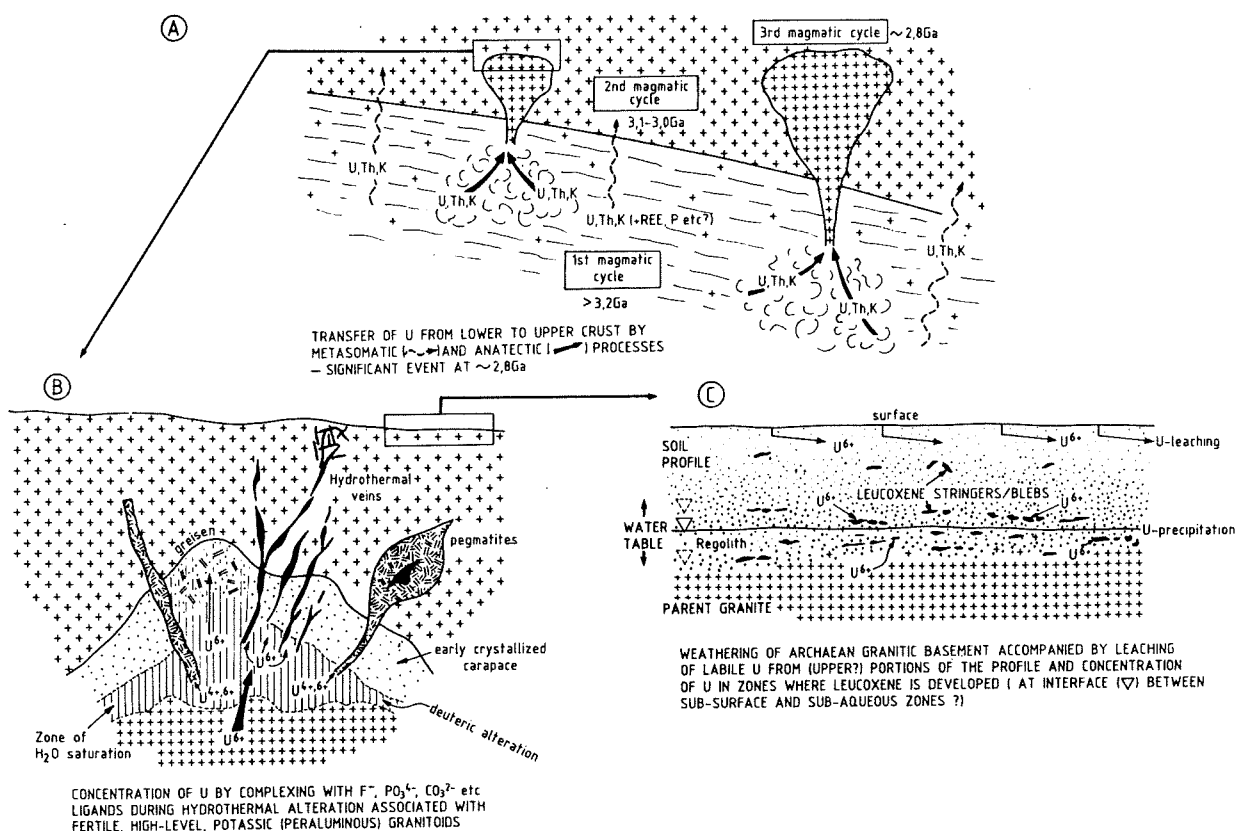


Figure 22: Schematic diagram depicting some of the principal factors responsible for the pattern of U and Th distribution in the Archaean granitic basement. These factors are also relevant in considerations regarding the origin of uranium in the Witwatersrand Basin.

prevail. Concentration of uranium into leucoxene, provision of labile uranium through the breakdown of most rock-forming minerals, a bulk source of detritus for arenaceous sedimentary accumulations (Button and Tyler, 1981), and an explanation for the apparent lack of "black sand" constituents such as magnetite and ilmenite are all features which may be explained by the existence of palaeosols in the Witwatersrand hinterland.

An explanation for the origin of uranium in the Witwatersrand Basin, whether it be regarded as placer or hydrothermal in origin, is probably less enigmatic than that for the origin of gold. This is because the degree of uranium enrichment in the basin is not as spectacular as it is for gold and, furthermore, uranium is a more ubiquitous component of the source area than is gold. In spite of this, no systematic explanation for the origin of uranium in the Witwatersrand reefs has yet been put forward, save that it must have been derived from a granitoid terrane. The present study, which examines the distribution of radioelements in the Archaean granitic crust as a function of the geology of the region, provides a framework within which more specific studies concerning uranium mineralization in the Witwatersrand Basin can be based. The diagrammatic summary presented in Figure 22 is not a model for the origin of uranium, but merely highlights some of the observations derived from this study which may be pertinent to the origin of Witwatersrand uranium mineralization. Regarded objectively, these observations do not militate against either the hydrothermal or placer concepts of mineralization but rather point to a gamut of processes involving aspects of both models. In all likelihood, processes such as the secular evolution of the Archaean crust, preconcentration of uranium during hydrothermal processes, redistribution of labile uranium in the palaeoweathering environment, the introduction of particulate uraninite, and the reconstitution of uranium during diagenesis, all played a role in the formation of the Witwatersrand deposits.

ACKNOWLEDGEMENTS

The Atomic Energy Corporation, in particular Dr. P D Toens and Dr. H J Brynard, are thanked for continued financial support, over a period of several years, which allowed this research to take place. Funding for this project was also derived from the CSIR-FRD. Professors D A Pretorius and C R Anhaeusser of the Economic Geology Research Unit, as well as Drs. R Hart and M Andreoli, Mr R Leahy and Mrs L de Matos of the Schonland Research Centre for Nuclear Sciences, are acknowledged for their logistical support and for numerous helpful discussions. The reactor staff at Pelindaba, in particular Messrs T Duncan, D Uitenbogaard, G Roux, E Jones and J McDonald, ably assisted with nuclear techniques. Several mining houses, including the Anglo American Corporation, Anglovaal Limited, General Mining Union Corporation, Gold Fields of South Africa, Johannesburg Consolidated Investment Company, and Rand Mines Limited, generously made many of their borehole intersections of the Archaean basement available for study. Finally, Janet Long, Barbara Schuble, Nuno Gomes and Richard Lewis are thanked for their capable secretarial and technical assistance. Two anonymous referees made suggestions which improved the quality of the manuscript.

REFERENCES

- Anhaeusser, C.R. (1973). The geology and geochemistry of the Archaean granites and gneisses of the Johannesburg-Pretoria dome. Spec. Publ. geol. Soc. S. Afr., 3, 261-385.
- Anhaeusser, C.R. (1977). Geological and geochemical investigations of the Roodekrans ultramafic complex and surrounding Archaean volcanic rocks, Krugersdorp district. Trans. geol. Soc. S.Afr., 80, 17-28.
- Anhaeusser, C.R. (1978). The geology and geochemistry of the Muldersdrift ultramafic complex and surrounding area, Krugersdorp district. Trans. geol. Soc. S. Afr., 81, 193-203.
- Anhaeusser, C.R. and Burger, A.J. (1982). An interpretation of U-Pb zircon ages for Archaean tonalite gneisses from the Johannesburg-Pretoria granite dome. Trans. geol. Soc. S. Afr., 85, 111-116.
- Anhaeusser, C.R. and Robb, L.J. (1981). Magmatic cycles and the evolution of the Archaean granitic crust in the eastern Transvaal and Swaziland. Spec. Publ. geol. Soc. Aust., 7, 457-467.
- Barton, J.M.Jr (1983). Isotopic constraints on possible tectonic models for crustal evolution in the Barberton granite-greenstone terrane, Southern Africa. Spec. Publ. geol. Soc. S. Afr., 9, 73-79.
- Barton, E.S.; Barton, J.M.Jr.; Callow, M.J.; Allsopp, H.L.; Evans, I.B. and Welke, H.J. (1986). Emplacement ages and implications for the source region of granitoid rocks associated with the Witwatersrand Basin. Ext. Abst. Geocongress '86, Geol. Soc. S. Afr., Johannesburg, 93-97.
- Barton, J.M.Jr.; Hunter, D.R.; Jackson, M.P.A. and Wilson, A.G. (1983). Geochronologic and Sr-isotopic studies of certain units in the Barberton granite-greenstone terrane, Swaziland. Trans. geol. Soc. S. Afr., 86, 71-80.
- Button, A. and Tyler, N. (1981). The character and economic significance of Precambrian palaeoweathering and erosion surfaces in southern Africa. Econ. Geol., 75th Anniv. Vol., 686-709.
- Cathelineau, M. (1987). U-Th-REE mobility during albitization and quartz dissolution in granitoids: evidence from south-east French Massif Centrale. Bull. Mineral., 110(2-3), 249-260.
- Condie, K.C. and Hunter, D.R. (1976). Trace element geochemistry of Archaean granitic rocks from the Barberton region, South Africa. Earth Planet. Sci. Lett. 29, 389-400.

- Corner, B.; Durrheim, R.J. and Nocolaysen, L.O. (1986). The structural framework of the Witwatersrand Basin as revealed by gravity and aeromagnetic data. Ext. Abstr. Geocongress '86, Geol. Soc. A. Afr., Johannesburg, pp 27-30.
- Cuney, M. and Friedrich, M. (1987). Physiochemical and crystal-chemical controls on accessory mineral paragenesis in granitoids: implications for uranium metallogenesis. Bull. Mineral., 110(2-3), 235-248.
- Drennan, G.R. (1988). The nature of the Archaean basement in the hinterland to the Welkom Goldfield. M.Sc. thesis (unpubl.) Univ. Witwatersrand, Johannesburg, 187pp.
- Drennan, G.R.; Meyer, M.; Robb, L.J. and Armstrong, R.A. (1988). A crustal profile in the Archaean basement west of the Welkom Goldfield; comparisons with the Vredefort crustal profile. Inform. Circ. Econ. geol. Res. Unit, Univ. Witwatersrand, Johannesburg, 199, 14pp.
- Feather, C.E. (1981). Some aspects of Witwatersrand mineralisation, with special reference to the uranium minerals. Prof. Paper U.S. Geol. Surv. 1161-Q, 23pp.
- Ferraz, M.F. (1989). The nature of the Archaean basement in the provenance areas of the East Rand and Evander Goldfields. M.Sc. thesis (unpubl.), Univ. Witwatersrand, Johannesburg, 145pp.
- Ferraz, M.F.; Robb, L.J. and Meyer, M. (1986). The nature of the Archaean basement in the provenance areas of the East Rand and Evander Goldfields. Ext. Abst. Geocongress '86, Geol. Soc. S. Afr., Johannesburg, 115-118.
- Ferraz, M.F.; Robb, L.J. and Meyer, M. (1987). Palaeoregolith profiles from the Archaean granitic basement and the possible origin of U-Ti phases in the Witwatersrand Basin. Ext. Abst. Int. Symp. Granites and Associated Mineralization, Salvador, Brazil, 279-281
- Grandstaff, D.E.; Edelman, M.J.; Foster, R.W.; Zbinden, E. and Kimberley, M.M. (1986). Chemistry and mineralogy of Precambrian palaeosols at the base of the Dominion and Pongola Groups (Transvaal, South Africa). Precambrian Res., 32, 97-131
- Hallbauer, D.K. (1981). Geochemistry and morphology of mineral components from the fossil gold and uranium placer of the Witwatersrand. Prof. Paper U.S. Geol. Surv., 1161-M, 22pp.
- Hallbauer, D.K. (1982). A review of some aspects of the geochemistry and mineralogy of the Witwatersrand gold deposits. Proc., 12th CMMI Congr. Ed. H.W. Glen. S. Afr. Inst. Min. Metall., Johannesburg, 957-964
- Hallbauer, D.K. (1984). Archaean granitic sources for the detrital mineral assemblage in Witwatersrand conglomerates. Abstr., Geocongr.'84, Geol. Soc. S. Afr., Potchefstroom, 53-56
- Hart, R.J.; Nicolayesen, L.O. and Gale, N.H. (1981). Radioelement concentrations in the deep profile through Precambrian basement of the Vredefort structure. J. Geophys. Res., 86 (B11), 10639-10652.
- Hiemstra, S.A. (1968). The mineralogy and petrology of the uraniferous conglomerates of the Dominion Reefs Mine, Klerksdorp area. Trans. geol. Soc. S. Afr., 71, 1-66.
- Holland, H.D. and Zbinden, E.A (1987). Palaeosols and the evolution of the atmosphere. (in press).
- Klemd, R. and Hallbauer, D.K (1987). Hydrothermally altered peraluminous Archaean granites as a provenance model for Witwatersrand sediments. Mineral. Deposita, 22, 227-235.
- Klemd, R.; Hallbauer, D.K. and Barton J.M.Jr. (1986). Styles of hydrothermal alteration in granitoid rocks along the northwestern margin of the Witwatersrand Basin. Ext. Abst. Geocongr.'86, Geol. Soc. S. Afr., Johannesburg, 149-154.
- Liebenberg, W.R. (1955). The occurrence of gold and radioactive minerals in the Witwatersrand System, the Dominion Reef, the Ventersdorp Contact Reef and the Black Reef. Trans. geol. Soc. S. Afr., 58, 101-223.
- Meyer, M. and Tainton, S. (1986). Characteristics of small pebble conglomerates in the Promise Formation of the West Rand Group. Ext. Abst. Geocongr. '86, Geol. Soc. S. Afr., Johannesburg, 155-160.
- Meyer, M.; Robb, L.J. and Anhaeusser, C.R. (1986). Uranium and thorium contents of Archaean granitoids from the Barberton Mountain Land, South Africa. Precambrian Res., 33, 303-321.
- Nicolayesen, L.O; Burger, A.J. and Liebenberg, W.R. (1962). Evidence for the extreme age of certain minerals from the Dominion Reef conglomerates and underlying granite in the Western Transvaal. Geochim. Cosmochim. Acta, 26, 15-24.
- Palmer, J.A. (1987). Palaeoweathering in the Witwatersrand and Ventersdorp Supergroups. M.Sc. thesis (unpubl.), Univ. Witwatersrand, Johannesburg, 140pp.
- Pretorius, D.A. (1986). Witwatersrand gold: the men, the money, the mineralization. Ext. Abstr. Geocongr. '86, Geol. Soc. S. Afr., Johannesburg, 1-4.

- Pretorius, D.A. (1976). The nature of the Witwatersrand gold-uranium deposits. In: K.H. Wolf Ed., Handbook of Stratabound and Stratiform Ore Deposits, VII. Elsevier, Amsterdam, 29-55.
- Ramdohr, P. (1957). Die "Pronto-Reaction". Neues Jb. Miner., 96, 217-222.
- Ramdohr, P. (1958). Die Uran- und Goldlagerstaetten Witwatersrand, Blind River District, Dominion Reef, Serra de Jacobina: erzmineralogische Untersuchungen und ein geologischer Vergleich. Abh. dt. Akad. Wiss., Berlin, 3, 33 pp.
- Robb, L.J. (1983). Geological and chemical characteristics of late granite plutons in the Barberton region and Swaziland with an emphasis on the Dalmein pluton - a review. Spec. Publ. geol. Soc. S. Afr., 9, 153-168.
- Robb, L.J. (1987). Fluid inclusion studies on hydrothermally altered granites from the Witwatersrand Basin hinterland. Abst. Fluid Inclusion Workshop, Bloemfontein, 2pp.
- Robb, L.J.; Davis, D.W. and Kamo, S. (1989). U-Pb ages on single detrital zircon grains from the Witwatersrand Basin: constraints on the age of sedimentation and on the evolution of granites adjacent to the depository. Inform. Circ. Econ. geol. Res. Unit, Univ. Witwatersrand, Johannesburg, 208, 16 pp.
- Robb, L.J. and Meyer, M. (1985). Uranium distribution and concentration mechanism in the hinterland of the Witwatersrand Basin. Ext. Abstr. Conf. on Concentration Mechanism of Uranium in Geological Environments, Nancy, France, 105-110.
- Robb, L.J. and Meyer, M. (1985). The nature of the Witwatersrand hinterland: conjectures on the source-area problem. Inform. Circ. Econ. geol. Res. Unit, Univ. Witwatersrand, Johannesburg, 178, 25pp.
- Sawka, W.N. and Chapell, B.W. (1986). The distribution of radioactive heat production in I- and S-type granites and residual source regions: implications to high heat flow areas in the Lachlan Fold belt, Australia. Aust. J. Earth Sci., 33, 107-118.
- Schidlowski, M. (1966). Beitraege zur Kenntnis der Radioaktiven Bestandteile der Witwatersrand-Konglomerate. II. Brannerit und "Uranpercherzgeister". Neues Jb. Miner., 105, 310-324.
- Slawson, W.F. (1976). Vredefort core: a cross-section of the upper crust?. Geochim. Cosmochim. Acta, 40, 117-121.
- Smith, N.D. and Minter, W.E.L. (1980). Sedimentological controls of gold and uranium in two Witwatersrand palaeoplacers. Econ. Geol., 75, 1-14.
- Smits, G. (1984). Some aspects of the uranium minerals in Witwatersrand sediments of the early Proterozoic. Precambrian Res., 25, 37-59.
- Vorwerk, R. (1984). Untersuchung von präkambrischen Graniten und Sedimentgesteinen mit Hilfe der Spaltspurmethode und der Alpha-Spektrometrie. Ph.D. thesis, (unpubl.) Univ. of Cologne, West Germany, 108pp.
- Wedepohl, K.H. (Ed.) (1969). Handbook of Geochemistry. Springer-Verlag, Berlin.
- Welke, H.J. and Nicolaysen, L.O. (1981). A new interpretive procedure for whole rock U-Pb systems, applied to the Vredefort crustal profile. J. Geophys. Res., 86(B11), 10681-10687.